

Higher-Order DGSEM Transport Calculations on Polytope Meshes for Massively-Parallel Architectures

Michael W. Hackemack

Chair: Jean C. Ragusa

Committee Members: Marvin L. Adams, Jim E. Morel, Nancy M. Amato

External Committee Member: Troy Becker

Department of Nuclear Engineering
Texas A&M University
College Station, TX, USA 77843
mike.hack@tamu.edu



Outline

1 Motivation

2 POLYFEM, a transport solver for arbitrary polygonal grids

- Linear Basis Functions on Polygons
- Quadratic Basis Functions on Polygons
- Results

3 DFEM Discretization of the Diffusion Equation

- Symmetric Interior Penalty Method
- Modified Interior Penalty Method
- Results

4 Thermal Neutron Upscattering Acceleration

- Overview of Methods
- IM1 Results

5 Conclusions and Open Items

Higher-Fidelity Transport Solutions

- Seek computational methods to more accurately and efficiently model radiation transport.
- Within the paradigm of Department of Energy's exascale initiative.
- Specifically focus on the use of unstructured meshes.



Topics of this Dissertation Work

Polygonal Finite Elements

- Seek basis functions compatible with arbitrary polygonal grids
 - Linear-completeness - $\{1, x, y\}$
 - Compatible with at least weakly-convex polygons
 - Seek a methodology to build higher-order basis functions
 - Investigate quadratic serendipity functions - $\{1, x, y, x^2, xy, y^2\}$
 - Still maintains weakly-convex compatibility

Diffusion Synthetic Acceleration (DSA)

- Seek a DFEM diffusion discretization for DSA
 - Stable and robust on arbitrary polytope grids
 - Efficiently solvable with suitable preconditioners
 - Scalable to massively-parallel problems
 - Seek a parallelizable thermal neutron upscattering acceleration method

The Continuous-Energy Transport Equation

Transport Equation

$$[\Omega \cdot \nabla + \sigma_t(\mathbf{r}, E)] \psi(\mathbf{r}, E, \Omega) = \int_{4\pi} \int_0^\infty \sigma_s(\mathbf{r}, E', E, \Omega', \Omega) \psi(\mathbf{r}, E', \Omega') dE' d\Omega' + Q(\mathbf{r}, E, \Omega)$$

Boundary Conditions

$$\psi(\mathbf{r}, E, \Omega) = \psi^{inc}(\mathbf{r}, E, \Omega) + \int_{\Omega' \cdot \mathbf{n} \geq 0}^{\infty} \int_0^{\infty} \beta(\mathbf{r}, E', E, \Omega', \Omega) \psi(\mathbf{r}, E', \Omega') dE' d\Omega'$$

Term Definitions

r - neutron position

E - neutron energy

Ω - neutron solid angle

$\psi(\mathbf{r}, E, \Omega)$ - angular flux

$Q(\mathbf{r}, E, \Omega)$ - distributed neutron source

$\sigma_t(\mathbf{r}, E)$ - total macroscopic cross section

$\sigma_s(\mathbf{r}, E', E, \Omega', \Omega)$ - total macroscopic scattering cross section

$\beta(\mathbf{r}, E', E, \Omega', \Omega)$ - boundary albedo

Multigroup DGFEM S_N Transport Equation

The multigroup S_N equations

$$\boldsymbol{\Omega}_m \cdot \nabla \psi_{m,g} + \sigma_{t,g} \psi_{m,g} = \sum_{g'=1}^G \sum_{n=0}^{N_g} \frac{2n+1}{4\pi} \sigma_{s,n}^{g' \rightarrow g} \sum_{k=-n}^n \phi_{g',n,k} Y_{n,k}(\boldsymbol{\Omega}_m) + Q_{m,g}$$

Multigroup DGFEM S_N Transport Equation

The multigroup S_N equations

$$\boldsymbol{\Omega}_m \cdot \nabla \psi_{m,g} + \sigma_{t,g} \psi_{m,g} = \sum_{g'=1}^G \sum_{n=0}^{N_g} \frac{2n+1}{4\pi} \sigma_{s,n}^{g' \rightarrow g} \sum_{k=-n}^n \phi_{g',n,k} Y_{n,k}(\boldsymbol{\Omega}_m) + Q_{m,g}$$

DGSEM spatial discretization

$$- (\boldsymbol{\Omega}_m \cdot \nabla b_m, \psi_m)_K + \left(\sigma_t b_m, \psi_m \right)_K + \sum_{f=1}^{N_f^K} \left\langle (\boldsymbol{\Omega}_m \cdot \mathbf{n}_f) b_m, \tilde{\psi}_m \right\rangle_f = (b_m, Q_m)_K$$

The upwind scheme

$$\tilde{\psi}_m(\mathbf{r}) = \begin{cases} \psi_m^-, & \partial K^+ \\ \psi_m^-, & \partial K^- \setminus \partial \mathcal{D} \\ \psi_m^{inc}, & \partial K^- \cap \partial \mathcal{D}^d \\ \psi_{m'}^-, & \partial K^- \cap \partial \mathcal{D}^r \end{cases} \quad \psi_m^\pm(\mathbf{r}) \equiv \lim_{s \rightarrow 0^\pm} \psi_m(\mathbf{r} + s(\boldsymbol{\Omega}_m \cdot \mathbf{n})\mathbf{n})$$

Iterative Procedure

Source Iteration

$$\begin{aligned}\psi^{(\ell+1)} &= \mathbf{L}^{-1} (\mathbf{M}\boldsymbol{\Sigma}\phi^{(\ell)} + \mathbf{Q}) \\ \phi^{(\ell+1)} &= \mathbf{D}\psi^{(\ell+1)}\end{aligned}$$

The operation \mathbf{L}^{-1} is a transport sweep.

Operator Terms

\mathbf{L} - streaming + collision operator

$\mathbf{L} = \text{diag}(L_1, \dots, L_{n_\Omega})$

\mathbf{M} - moment-to-discrete operator

\mathbf{D} - discrete-to-moment operator

$\boldsymbol{\Sigma}$ - scattering operator

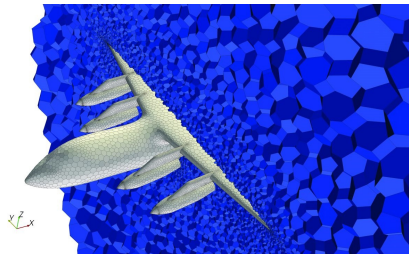
\mathbf{Q} - source operator

Flux Moment Equivalent Linear System

$$(\mathbf{I} - \mathbf{D}\mathbf{L}^{-1}\mathbf{M}\boldsymbol{\Sigma})\Phi = \mathbf{D}\mathbf{L}^{-1}\mathbf{Q}$$

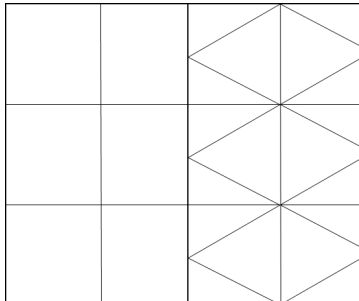
Polytope Meshes

- Other physics communities are now employing polytope grids due to decreased cell/face counts (CFD and solid mechanics in particular)
- They allow for transition elements between different domain regions
- Hanging nodes from non-conforming meshes are not necessary
- Independently-generated simplicial grids (*i.e.* created in parallel) can be stitched together with polytopes without communicating the whole mesh across processors



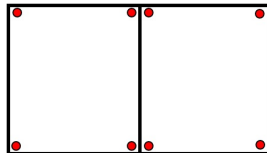
Polytope Meshes

- Other physics communities are now employing polytope grids due to decreased cell/face counts (CFD and solid mechanics in particular)
- They allow for transition elements between different domain regions
- Hanging nodes from non-conforming meshes are not necessary
- Independently-generated simplicial grids (*i.e.* created in parallel) can be stitched together with polytopes without communicating the whole mesh across processors

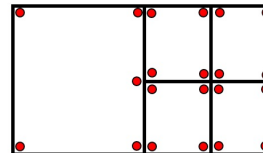


Polytope Meshes

- Other physics communities are now employing polytope grids due to decreased cell/face counts (CFD and solid mechanics in particular)
- They allow for transition elements between different domain regions
- Hanging nodes from non-conforming meshes are not necessary
- Independently-generated simplicial grids (*i.e.* created in parallel) can be stitched together with polytopes without communicating the whole mesh across processors



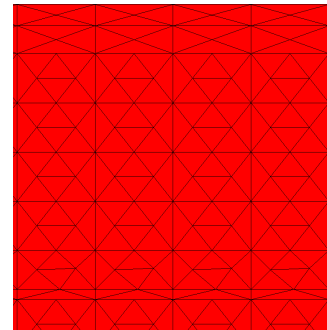
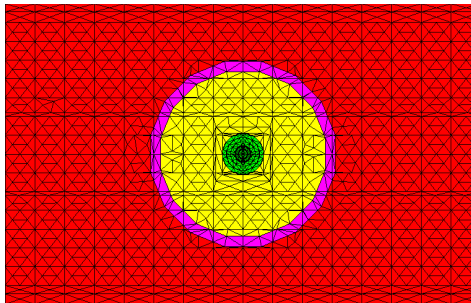
(a)



(b)

Polytope Meshes

- Other physics communities are now employing polytope grids due to decreased cell/face counts (CFD and solid mechanics in particular)
- They allow for transition elements between different domain regions
- Hanging nodes from non-conforming meshes are not necessary
- Independently-generated simplicial grids (*i.e.* created in parallel) can be stitched together with polytopes without communicating the whole mesh across processors



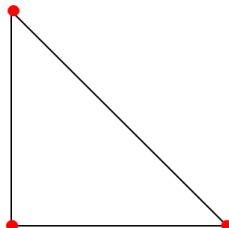
Higher-Order FEM Basis Functions

- More processor work per element solve in transport sweep.
- Increased convergence rates:

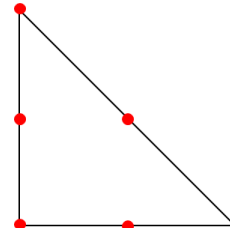
$$\|u - u_h\|_{L_2} = C h^q, \quad \|u - u_h\|_{L_2} = C N_{dof}^{-\frac{q}{d}}$$

$$q = \min(p + 1, r)$$

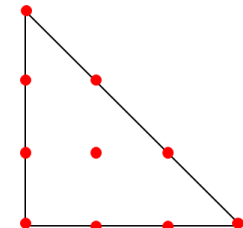
r - solution regularity



Linear



Quadratic



Cubic



Diffusion Synthetic Acceleration

Source Iteration Approximate Spectral Radius

$$\rho^{(k+1)} \approx \frac{||\phi^{(k+1)} - \phi^{(k)}||}{||\phi^{(k)} - \phi^{(k-1)}||}$$

Optically Thick Cases - leakage/absorption does not dominate

- $\sigma_s^{g \rightarrow g} / \sigma_{t,g} \approx 1$ and $(\sigma_{t,g} \cdot \text{diam}(\mathcal{D})) \gg 1$
- Thermal upscattering into higher energy groups is significant

Answer - Precondition the transport sweep

- Diffusion Synthetic Acceleration (DSA)
- Transport Synthetic Acceleration (TSA)
- Boundary Projection Acceleration (BPA)
- etc.

Diffusion Synthetic Acceleration

Source Iteration Approximate Spectral Radius

$$\rho^{(k+1)} \approx \frac{||\phi^{(k+1)} - \phi^{(k)}||}{||\phi^{(k)} - \phi^{(k-1)}||}$$

Optically Thick Cases - leakage/absorption does not dominate

- $\sigma_s^{g \rightarrow g} / \sigma_{t,g} \approx 1$ and $(\sigma_{t,g} \cdot \text{diam}(\mathcal{D})) \gg 1$
- Thermal upscattering into higher energy groups is significant

Answer - Precondition the transport sweep

- Diffusion Synthetic Acceleration (DSA)
- Transport Synthetic Acceleration (TSA)
- Boundary Projection Acceleration (BPA)
- etc.

Finite element architecture

Mass Matrix - element K

$$\mathbf{M}^K = \int_K d\mathbf{r} \lambda(\mathbf{x}) \lambda^T(\mathbf{x}) = \sum_{q=1}^{N_q^K} w_q^K \lambda(\mathbf{x}_q^K) \lambda^T(\mathbf{x}_q^K)$$

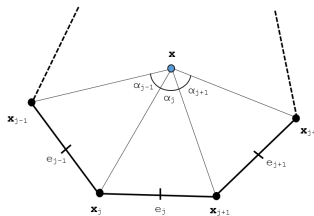
Advection Matrix - element K

$$\mathbf{G}^K = \int_K d\mathbf{r} \nabla \lambda(\mathbf{x}) \lambda^T(\mathbf{x}) = \sum_{q=1}^{N_q^K} w_q^K \nabla \lambda(\mathbf{x}_q^K) \lambda^T(\mathbf{x}_q^K)$$

Surface Matrix - face f for element K

$$\mathbf{N}_f^K = \int_f ds \lambda(\mathbf{x}) \lambda^T(\mathbf{x}) = \sum_{q=1}^{N_f} w_q^f \lambda(\mathbf{x}_q^f) \lambda^T(\mathbf{x}_q^f)$$

Linear Basis Functions - Generalized Barycentric Coordinates



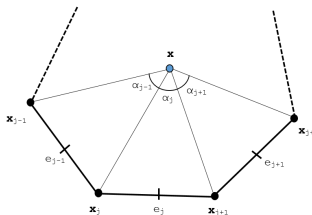
Basis Function Properties - Barycentric Coordinates

λ_i - linear basis function located at vertex i

- ① Positivity*: $\lambda_i \geq 0$
- ② Partition of Unity: $\sum_i \lambda_i = 1$
- ③ Affine combination: $\sum_i \mathbf{x}_i \lambda_i(\mathbf{x}) = \mathbf{x}$
- ④ Lagrange property: $\lambda_i(\mathbf{x}_j) = \delta_{ij}$
- ⑤ Piecewise boundary linearity: $\lambda_j((1 - \mu)\mathbf{x}_j + \mu\mathbf{x}_{j+1}) = (1 - \mu)\lambda_j(\mathbf{x}_j) + \mu\lambda_j(\mathbf{x}_{j+1})$

*convex polygons

Linear Basis Functions - Generalized Barycentric Coordinates

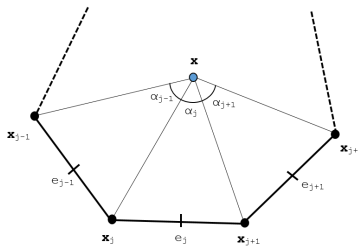


Linear basis functions that we consider

- ① Wachspress rational coordinates*
- ② Piecewise linear (PWL) coordinates*
- ③ Mean value coordinates
- ④ Maximum entropy coordinates

*have been previously analyzed for transport problems

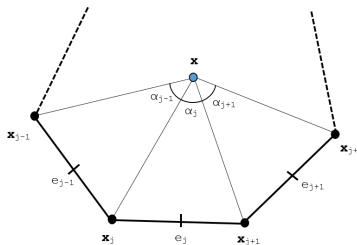
Wachspress Rational Functions



$$\lambda_i^W(\mathbf{x}) = \frac{w_i(\mathbf{x})}{\sum_j w_j(\mathbf{x})}, \quad w_j(\mathbf{x}) = \frac{A(\mathbf{x}_{j-1}, \mathbf{x}_j, \mathbf{x}_{j+1})}{A(\mathbf{x}, \mathbf{x}_{j-1}, \mathbf{x}_j) A(\mathbf{x}, \mathbf{x}_j, \mathbf{x}_{j+1})}$$

$$A(\mathbf{x}_1, \mathbf{x}_2, \mathbf{x}_3) = \frac{1}{2} \begin{vmatrix} 1 & 1 & 1 \\ x_1 & x_2 & x_3 \\ y_1 & y_2 & y_3 \end{vmatrix}$$

Piecewise Linear (PWL) Functions



$$\lambda_i^{PWL}(\mathbf{x}) = t_i(\mathbf{x}) + \alpha_i t_c(\mathbf{x})$$

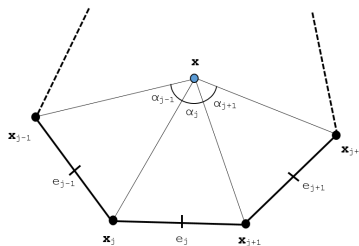
t_i - standard 2D linear function for a triangle $(i, i + 1, C)$; 1 at vertex i that linearly decreases to 0 to the cell center and the adjoining vertices

t_c - 2D tent function; 1 at cell center and linearly decreases to 0 to each cell vertex

$\alpha_i = \frac{1}{N_V}$ - weight parameter for vertex i

N_V - number of cell vertices

Mean Value (MV) Coordinates

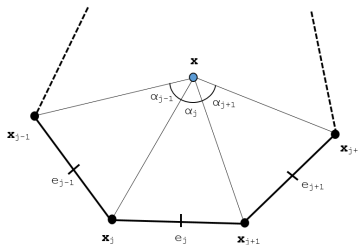


$$\lambda_i^{MV}(\mathbf{x}) = \frac{w_i(\mathbf{x})}{\sum_j w_j(\mathbf{x})}, \quad w_j(\mathbf{x}) = \frac{\tan(\alpha_{j-1}/2) + \tan(\alpha_j/2)}{|\mathbf{x}_j - \mathbf{x}|}$$

Limit as $\mathbf{x} \rightarrow \mathbf{x}_j$

$$\lim_{\mathbf{x} \rightarrow \mathbf{x}_j} \tan(\alpha_{j-1}/2) + \tan(\alpha_j/2) = 0 \quad \rightarrow \quad \lim_{\mathbf{x} \rightarrow \mathbf{x}_j} w_j(\mathbf{x}) = 1$$

Maximum Entropy (ME) Coordinates



$$\lambda_i^{ME}(\mathbf{x}) = \frac{w_i(\mathbf{x})}{\sum_j w_j(\mathbf{x})}, \quad w_j(\mathbf{x}) = m_j(\mathbf{x}) \exp(-\omega^* \cdot (\mathbf{x}_j - \mathbf{x}))$$

$$\mathcal{L}(\lambda, \omega_0, \omega) = - \sum_i \lambda_i(\mathbf{x}) \ln \left(\frac{\lambda_i(\mathbf{x})}{m_i(\mathbf{x})} \right) - \omega_0 \left(\sum_i \lambda_i(\mathbf{x}) - 1 \right) - \omega \cdot \left(\sum_i \lambda_i(\mathbf{x}) (\mathbf{x}_i - \mathbf{x}) \right)$$

Summary of the Linear Basis Functions

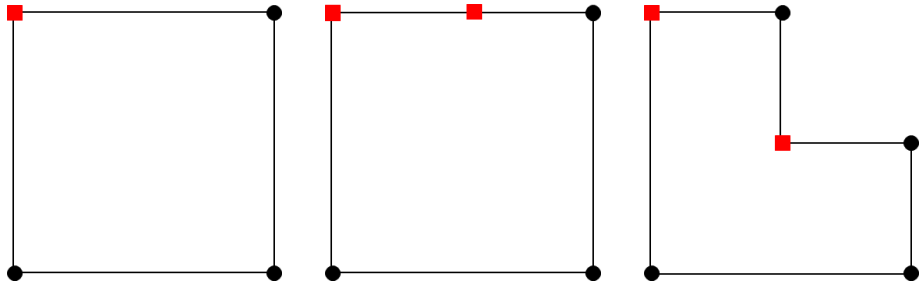
Basis Function	Dimension	Polytope Types	Integration	Direct/Iterative
Wachspress	2D/3D	Convex*	Numerical	Direct
PWL	1D/2D/3D	Convex/Concave	Analytical	Direct
Mean Value	2D**	Convex/Concave	Numerical	Direct
Max Entropy	1D/2D/3D	Convex/Concave	Numerical	Iterative***

* - weak convexity for Wachspress coordinates does not cause blow up

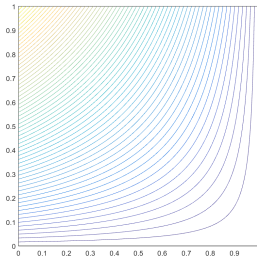
** - mean value 3D analogue only applicable triangular-faceted polyhedra

*** - maximum entropy minimization solved via Newton's Method

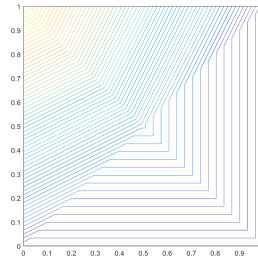
Basis Function Locations



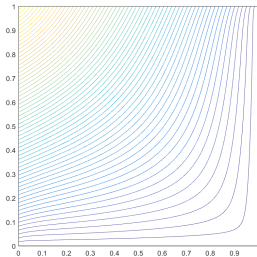
Basis Functions on the Unit Square



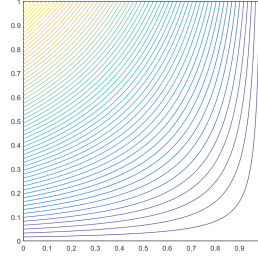
Wachspress



PWL

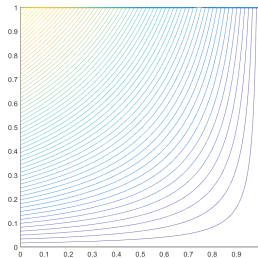


Mean Value

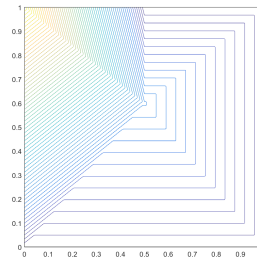


Maximum Entropy

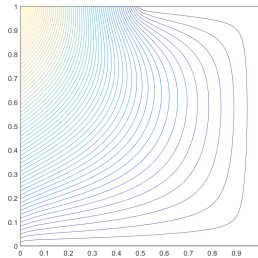
Basis Functions on the Degenerate Pentagon



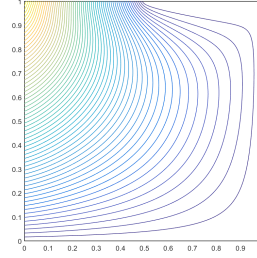
Wachspress



PWL

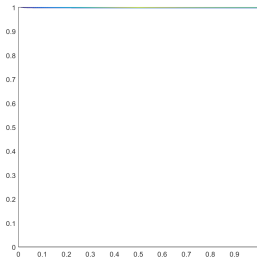


Mean Value

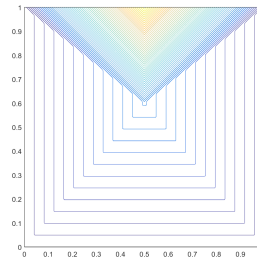


Maximum Entropy

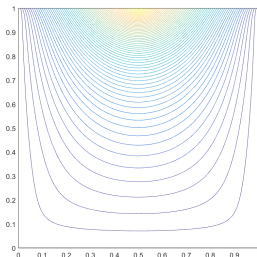
Basis Functions on the Degenerate Pentagon



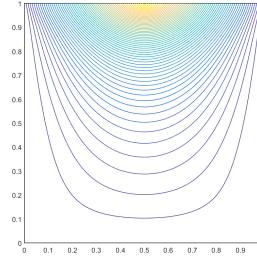
Wachspress



PWL

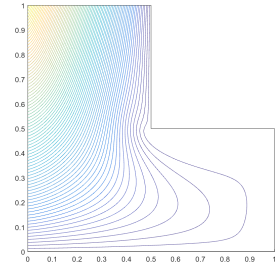
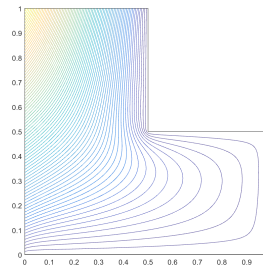
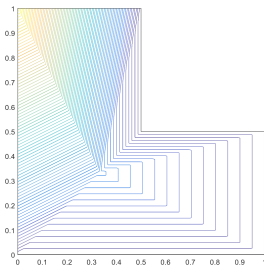
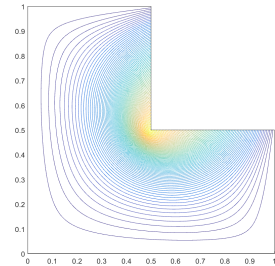
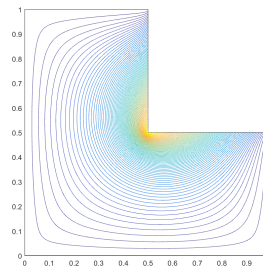
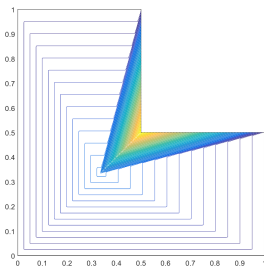


Mean Value



Maximum Entropy

Basis Functions on the L-Shaped Domain

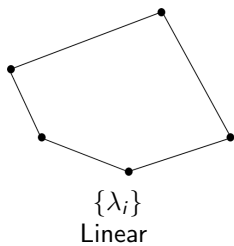


PWL

Mean Value

Quadratic Serendipity Basis Functions on 2D Polygons [1]

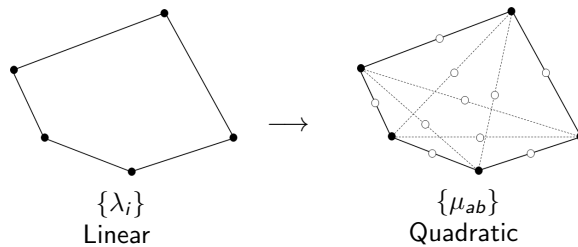
- ① Form the linear barycentric functions - $\{\lambda_i\}$
- ② Construct the pairwise products - $\{\mu_{ab}\}$
- ③ Eliminate the interior nodes to form a serendipity basis - $\{\xi_{ij}\}$



[1] A. Rand, A. Gillette, and C. Bajaj, "Quadratic serendipity finite elements on polygons using generalized barycentric coordinates," *Mathematics of computation*, **83**, 290, 2691-2716 (2014).

Quadratic Serendipity Basis Functions on 2D Polygons [1]

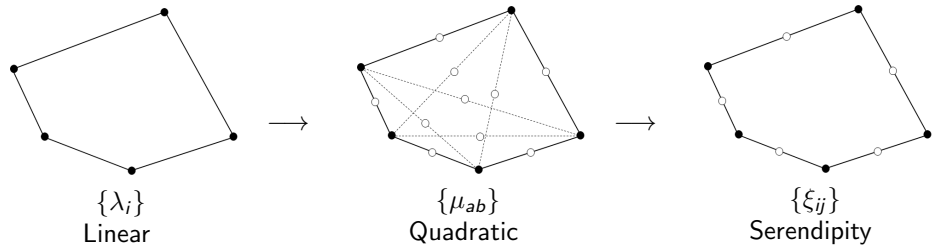
- ① Form the linear barycentric functions - $\{\lambda_i\}$
- ② Construct the pairwise products - $\{\mu_{ab}\}$
- ③ Eliminate the interior nodes to form a serendipity basis - $\{\xi_{ij}\}$



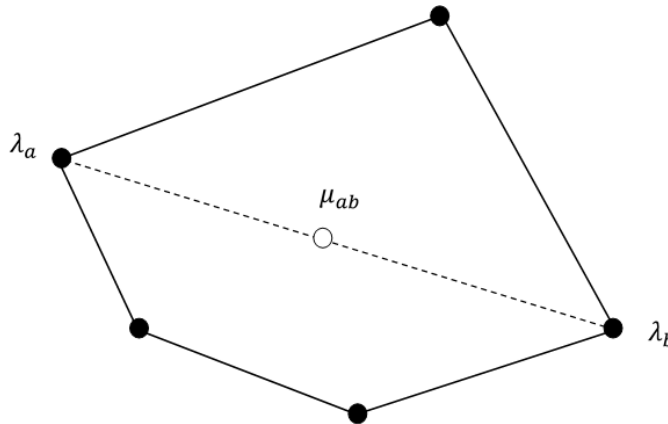
[1] A. Rand, A. Gillette, and C. Bajaj, "Quadratic serendipity finite elements on polygons using generalized barycentric coordinates," *Mathematics of computation*, **83**, 290, 2691-2716 (2014).

Quadratic Serendipity Basis Functions on 2D Polygons [1]

- ① Form the linear barycentric functions - $\{\lambda_i\}$
 - ② Construct the pairwise products - $\{\mu_{ab}\}$
 - ③ Eliminate the interior nodes to form a serendipity basis - $\{\xi_{ij}\}$



[1] A. Rand, A. Gillette, and C. Bajaj, "Quadratic serendipity finite elements on polygons using generalized barycentric coordinates," *Mathematics of computation*, **83**, 290, 2691-2716 (2014).

Pairwise products of the barycentric basis functions - $\mu_{ab} = \lambda_a \lambda_b$ 

Pairwise products of the barycentric basis functions - $\mu_{ab} = \lambda_a \lambda_b$

Necessary Constraints - by construction

$$\sum_{aa \in V} \mu_{aa} + \sum_{ab \in E \cup D} 2\mu_{ab} = 1$$

 V - vertex nodes E - face midpoint nodes D - interior diagonal nodes

$$\sum_{a \in V} \mathbf{x}_a \mu_{aa} + \sum_{ab \in E \cup D} 2\mathbf{x}_{ab} \mu_{ab} = \mathbf{x}$$

$$V + E + D = n + n + \frac{n(n-3)}{2}$$

$$\sum_{a \in V} \mathbf{x}_a \mathbf{x}_a^T \mu_{aa} + \sum_{ab \in E \cup D} (\mathbf{x}_a \mathbf{x}_b^T + \mathbf{x}_b \mathbf{x}_a^T) \mu_{ab} = \mathbf{x} \mathbf{x}^T$$

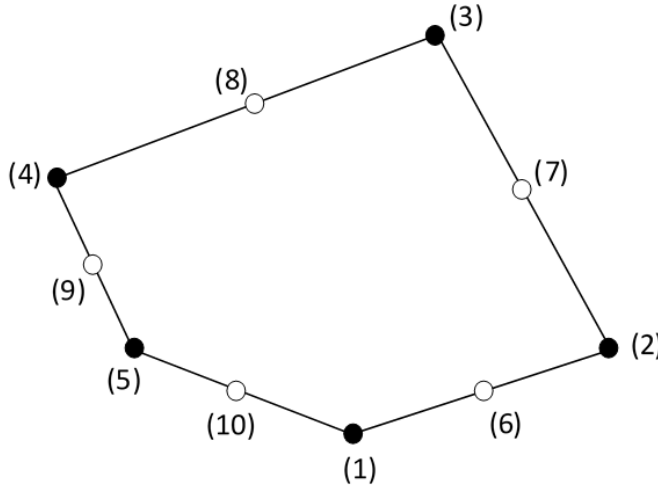
$$V + E + D = \frac{n(n+1)}{2} = N_q$$

Further Notation/Notes

$$\mathbf{x}_{ab} = \frac{\mathbf{x}_a + \mathbf{x}_b}{2}, \quad \mu_{ab} = \lambda_a \lambda_b$$

$$\mu_{ab}^K(\mathbf{r}) = 0, \quad \{ab \in D, \mathbf{r} \in \partial K\}$$

Eliminate interior nodes to form Serendipity basis



Eliminate interior nodes to form Serendipity basis

Necessary Serendipity Constraints

$$\sum_{ii \in V} \xi_{ii} + \sum_{i(i+1) \in E} 2\xi_{i(i+1)} = 1$$

ξ_{ii} - basis function at vertex i

$$\sum_{ii \in V} \mathbf{x}_{ii} \xi_{ii} + \sum_{i(i+1) \in E} 2\mathbf{x}_{i(i+1)} \xi_{i(i+1)} = \mathbf{x}$$

$\xi_{i(i+1)}$ - basis function at face midpoint between vertices $(i, i + 1)$

$$\sum_{ii \in V} \mathbf{x}_i \mathbf{x}_i^T \xi_{ii} + \sum_{i(i+1) \in E} \left(\mathbf{x}_i \mathbf{x}_{i+1}^T + \mathbf{x}_{i+1} \mathbf{x}_i^T \right) \xi_{i(i+1)} = \mathbf{x} \mathbf{x}^T$$

Reduction Problem - $[\xi] := \mathbb{A} [\mu]$

$$\mathbb{A} = \begin{bmatrix} c_{11}^{11} & \dots & c_{ab}^{11} & \dots & c_{(n-2)n}^{11} \\ \vdots & \ddots & \vdots & \ddots & \vdots \\ c_{11}^{ij} & \dots & c_{ab}^{ij} & \dots & c_{(n-2)n}^{ij} \\ \vdots & \ddots & \vdots & \ddots & \vdots \\ c_{11}^{n(n+1)} & \dots & c_{ab}^{n(n+1)} & \dots & c_{(n-2)n}^{n(n+1)} \end{bmatrix}$$

Eliminate interior nodes to form Serendipity basis

Reduction Problem

- Each serendipity function is formed by its corresponding quadratic function plus linear combinations of the diagonal functions
- Simplified matrix form:

$$\mathbb{A} = [\mathbb{I} \mid \mathbb{A}']$$

\mathbb{I} - $(2n \times 2n)$ identity matrix

\mathbb{A}' - $(2n \times \frac{n(n-3)}{2})$ constraint matrix

Column ab of \mathbb{A}' : underdetermined system - $\mathbb{B}\mathbf{c}_{ab} = \mathbf{q}_{ab}$

$$\sum_{ii \in V} c_{ab}^{ii} + \sum_{i(i+1) \in E} 2c_{ab}^{i(i+1)} = 2$$

$$\sum_{ii \in V} c_{ab}^{ii} \mathbf{x}_{ii} + \sum_{i(i+1) \in E} 2c_{ab}^{i(i+1)} \mathbf{x}_{i(i+1)} = 2\mathbf{x}_{ab}$$

$$\sum_{ii \in V} c_{ab}^{ii} \mathbf{x}_i \mathbf{x}_i^T + \sum_{i(i+1) \in E} c_{ab}^{i(i+1)} \left(\mathbf{x}_i \mathbf{x}_{i+1}^T + \mathbf{x}_{i+1} \mathbf{x}_i^T \right) = \mathbf{x}_a \mathbf{x}_b^T + \mathbf{x}_b \mathbf{x}_a^T$$

Eliminate interior nodes to form Serendipity basis

Reduction Problem

- Each serendipity function is formed by its corresponding quadratic function plus linear combinations of the diagonal functions
- Simplified matrix form:

$$\mathbb{A} = [\mathbb{I} \mid \mathbb{A}']$$

\mathbb{I} - $(2n \times 2n)$ identity matrix

\mathbb{A}' - $(2n \times \frac{n(n-3)}{2})$ constraint matrix

Column ab of \mathbb{A}' : underdetermined system - $\mathbb{B}\mathbf{c}_{ab} = \mathbf{q}_{ab}$

$$\sum_{ii \in V} c_{ab}^{ii} + \sum_{i(i+1) \in E} 2c_{ab}^{i(i+1)} = 2$$

$$\sum_{ii \in V} c_{ab}^{ii} \mathbf{x}_{ii} + \sum_{i(i+1) \in E} 2c_{ab}^{i(i+1)} \mathbf{x}_{i(i+1)} = 2\mathbf{x}_{ab}$$

$$\sum_{ii \in V} c_{ab}^{ii} \mathbf{x}_i \mathbf{x}_i^T + \sum_{i(i+1) \in E} c_{ab}^{i(i+1)} \left(\mathbf{x}_i \mathbf{x}_{i+1}^T + \mathbf{x}_{i+1} \mathbf{x}_i^T \right) = \mathbf{x}_a \mathbf{x}_b^T + \mathbf{x}_b \mathbf{x}_a^T$$

Special case - bilinear coordinates on the unit square

Bilinear coordinates and quadratic extension

$$\lambda_1 = (1-x)(1-y)$$

$$\lambda_2 = x(1-y)$$

$$\lambda_3 = xy$$

$$\lambda_4 = (1-x)y$$

$$\mu_{11} = (1-x)^2(1-y)^2 \quad \mu_{12} = (1-x)x(1-y)^2$$

$$\mu_{22} = x^2(1-y)^2 \quad \mu_{23} = x^2y(1-y)$$

$$\mu_{33} = x^2y^2 \quad \mu_{34} = (1-x)xy^2$$

$$\mu_{44} = (1-x)^2y^2 \quad \mu_{41} = (1-x)^2y(1-y)$$

$$\mu_{13} = (1-x)x(1-y)y \quad \mu_{24} = (1-x)x(1-y)y$$

Reduction matrix

$$\mathbb{A} = \begin{bmatrix} 1 & 0 & 0 & 0 & 0 & 0 & 0 & 0 & -1 & 0 \\ 0 & 1 & 0 & 0 & 0 & 0 & 0 & 0 & 0 & -1 \\ 0 & 0 & 1 & 0 & 0 & 0 & 0 & 0 & -1 & 0 \\ 0 & 0 & 0 & 1 & 0 & 0 & 0 & 0 & 0 & -1 \\ 0 & 0 & 0 & 0 & 1 & 0 & 0 & 0 & 1/2 & 1/2 \\ 0 & 0 & 0 & 0 & 0 & 1 & 0 & 0 & 1/2 & 1/2 \\ 0 & 0 & 0 & 0 & 0 & 0 & 1 & 0 & 1/2 & 1/2 \\ 0 & 0 & 0 & 0 & 0 & 0 & 0 & 1 & 1/2 & 1/2 \end{bmatrix}$$

Serendipity coordinates

$$\xi_{11} = (1-x)(1-y)(1-x-y)$$

$$\xi_{22} = x(1-y)(x-y)$$

$$\xi_{33} = xy(-1+x+y)$$

$$\xi_{44} = (1-x)y(y-x)$$

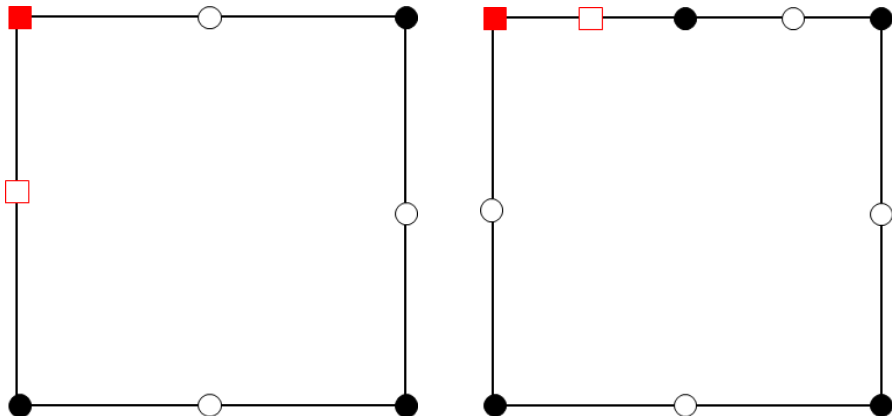
$$\xi_{12} = (1-x)x(1-y)$$

$$\xi_{23} = xy(1-y)$$

$$\xi_{34} = (1-x)xy$$

$$\xi_{41} = (1-x)y(1-y)$$

Basis Function Locations



Motivation
○○○○○○○○

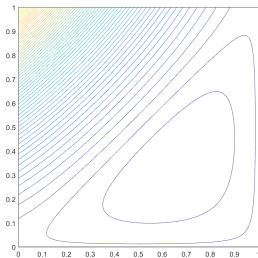
POLYFEM
○○○○○○○○○○●○○○○○○

MIP Form
○○○○○○○○○○

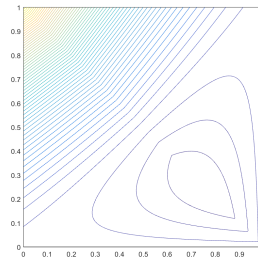
Upscattering Acceleration
○○○○○○○○○○○○

Conclusions and Open Items
○○○

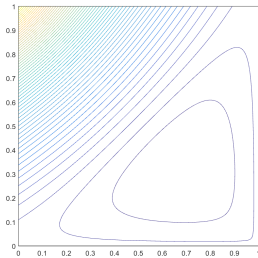
Quadratic Basis Functions on the Unit Square



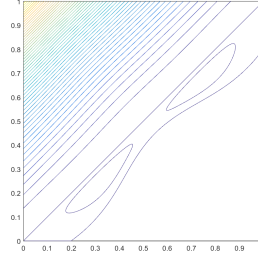
Wachspress



PWL



Mean Value



Maximum Entropy

Motivation
○○○○○○○○

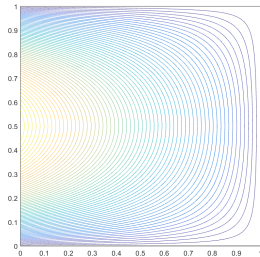
POLYFEM
○○○○○○○○○○●○○○○○○

MIP Form
○○○○○○○○○○

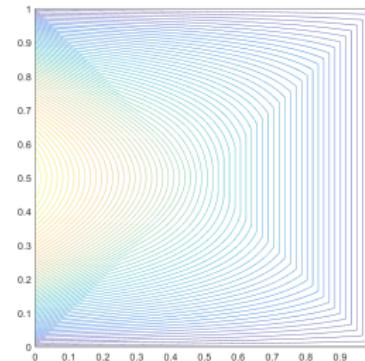
Upscattering Acceleration
○○○○○○○○○○○○

Conclusions and Open Items
○○○

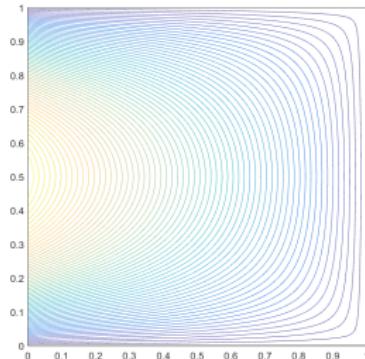
Quadratic Basis Functions on the Unit Square



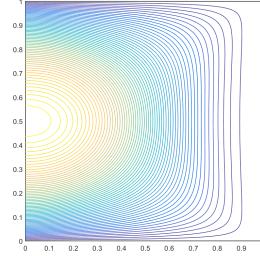
Wachspress



PWL



Mean Value



Maximum Entropy

Motivation
○○○○○○○○

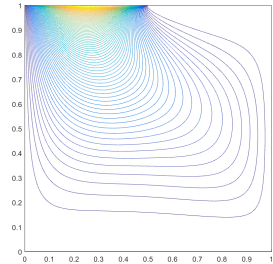
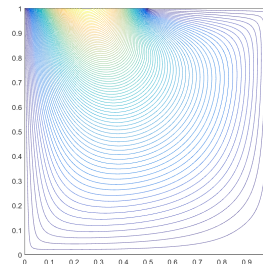
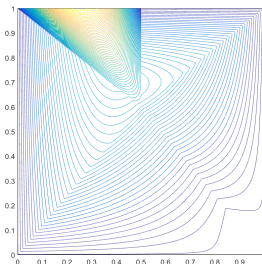
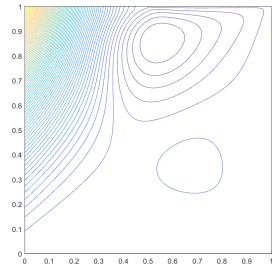
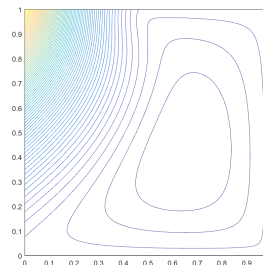
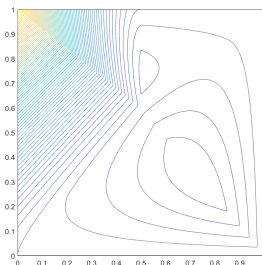
POLYFEM
○○○○○○○○○○●○○○○○

MIP Form
○○○○○○○○○○

Upscattering Acceleration
○○○○○○○○○○○○

Conclusions and Open Items
○○○

Quadratic Basis Functions on the Degenerate Pentagon



PWL

Mean Value

Maximum Entropy



Results Summary

- ① Linear basis functions capture exactly-linear transport solutions.
- ② Quadratic basis functions capture exactly-quadratic transport solutions.
- ③ Convergence rate analysis using the Method of Manufactured Solutions.
- ④ Convergence rate analysis bound by the solution regularity.
- ⑤ Linear and quadratic basis functions capture the thick diffusion limit.

Exactly-Linear Transport Solutions

MMS Solution

$$\mu \frac{\partial \psi}{\partial x} + \eta \frac{\partial \psi}{\partial y} + \sigma_t \psi = Q(x, y, \mu, \eta)$$

$$\psi(x, y, \mu, \eta) = ax + by + c\mu + d\eta + e$$

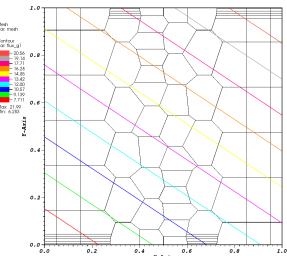
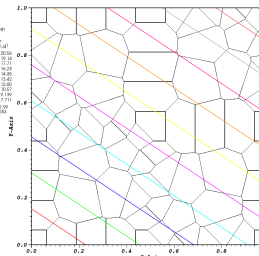
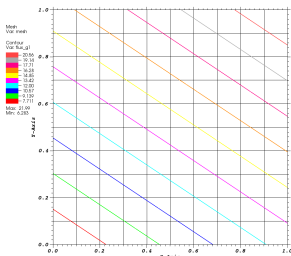
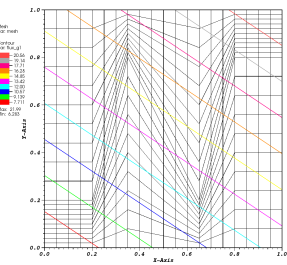
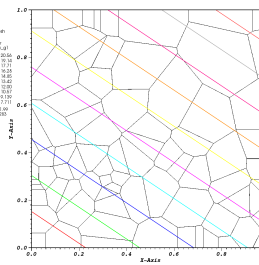
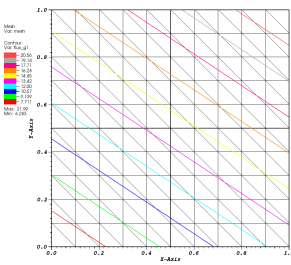
$$\phi(x, y) = 2\pi(ax + by + e)$$

Forcing Function

$$Q(x, y, \mu, \eta) = a\mu + b\eta + \sigma_t(c\mu + d\eta) + \sigma_t(ax + by + e)$$

$$\sigma_t = a = c = d = e = 1.0 \quad b = 1.5$$

Exactly-Linear Transport Solutions - linear PWL



Exactly-Quadratic Transport Solutions

$$\{1, x, y, x^2, xy, y^2\}$$

$$\psi_q(x, y, \mu, \eta) = a + bx + cy + dxy + ex^2 + fy^2$$

$$\phi_q(x, y) = 2\pi (a + bx + cy + dxy + ex^2 + fy^2)$$

- $L_x = L_y = 1.0$
- $\sigma_t = a = b = c = d = e = f = 1.0$
- Quadratic serendipity functions span space

$$\{1, x, y, x^2, xy, y^2, x^2y, xy^2, x^2y^2\}$$

$$\psi_{x2y2}(x, y, \mu, \eta) = x(L_x - x)y(L_y - y)$$

$$\phi_{x2y2}(x, y) = 2\pi x(L_x - x)y(L_y - y)$$

- $L_x = L_y = 1.0$
- Quadratic serendipity functions do NOT span space

{1, x, y, x^2 , xy, y^2 }

Mesh Type	Basis Functions			
	Wachspress	PWL	Mean Value	Max. Entropy
Cartesian	2.23e-13	7.25e-13	5.68e-14	5.65e-14
Triangular	7.85e-14	1.46e-13	2.52e-14	2.54e-13
Shes. Poly	1.14e-14	6.82e-14	5.75e-14	1.25e-13
Sine Poly	2.56e-13	4.15e-13	3.25e-13	6.37e-13
Z-Poly	5.24e-14	5.35e-14	1.68e-13	5.19e-14
Z-Quad	6.64e-14	4.42e-14	8.29e-14	6.82e-13

$$\{1, x, y, x^2, xy, y^2, x^2y, xy^2, x^2y^2\}$$

Mesh Type	Basis Functions			
	Wachspress	PWL	Mean Value	Max. Entropy
Cartesian	3.50e-06	2.72e-05	8.29e-06	3.86e-05
Triangular	5.13e-05	5.13e-05	5.13e-05	5.13e-05
Shes. Poly	3.97e-04	3.37e-04	2.81e-04	3.91e-04
Sine Poly	3.75e-05	1.22e-04	7.62e-05	1.39e-04
Z-Poly	2.93e-05	3.07e-05	2.59e-05	3.46e-05
Z-Quad	2.98e-05	8.73e-05	5.08e-05	1.17e-04

Convergence Rate Analysis by MMS

Sinusoid Solution

$$\psi_s(x, y) = \sin\left(\nu \frac{\pi x}{L_x}\right) \sin\left(\nu \frac{\pi y}{L_y}\right)$$

$$\phi_s(x, y) = 2\pi \sin\left(\nu \frac{\pi x}{L_x}\right) \sin\left(\nu \frac{\pi y}{L_y}\right)$$

- Cartesian, triangular and Voronoi polygon meshes
- Wachspress, PWL, MV, and MAXENT

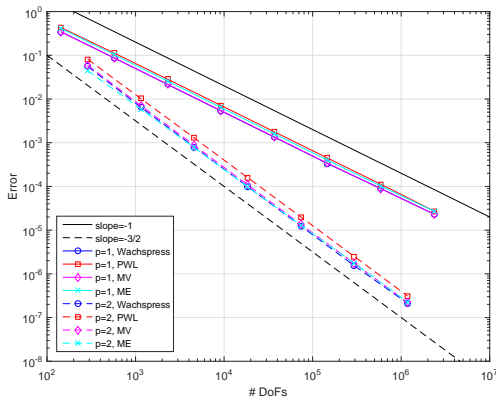
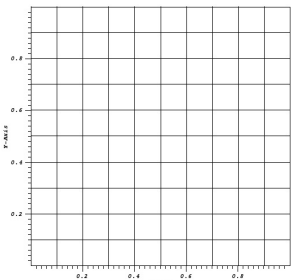
Localized Gaussian Solution

$$\psi_g(x, y) = \frac{x(L_x - x)}{L_x^2} \frac{y(L_y - y)}{L_y^2} \exp\left(-\frac{(x - x_0)^2 + (y - y_0)^2}{L_x L_y}\right)$$

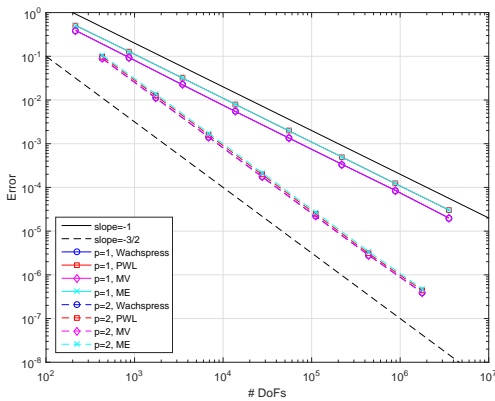
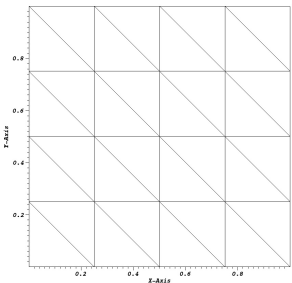
$$\phi_g(x, y) = 2\pi \frac{x(L_x - x)}{L_x^2} \frac{y(L_y - y)}{L_y^2} \exp\left(-\frac{(x - x_0)^2 + (y - y_0)^2}{L_x L_y}\right)$$

- Use spatial Adaptive Mesh Refinement (AMR)
- PWL, MV, and MAXENT

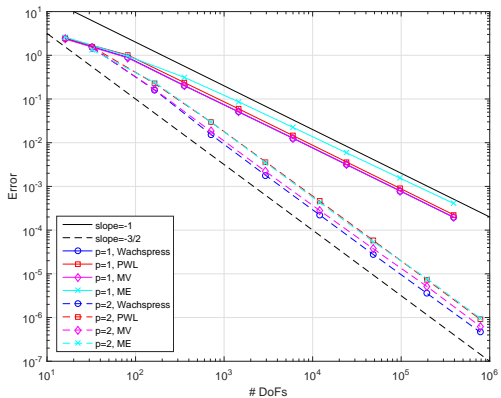
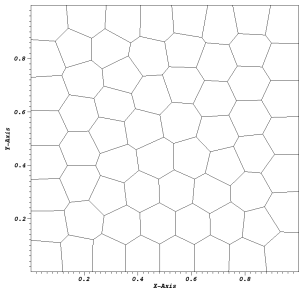
Cartesian Sinusoid MMS Results



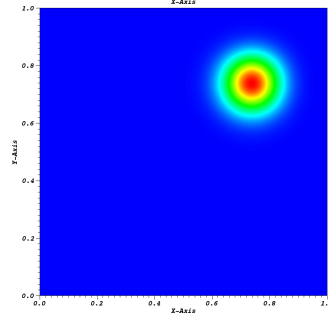
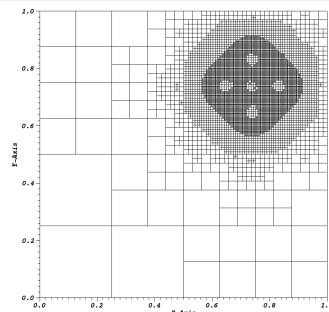
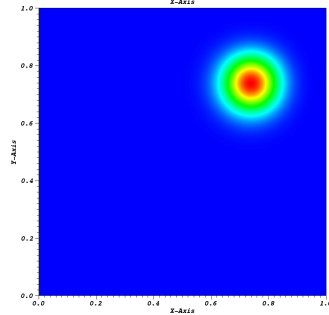
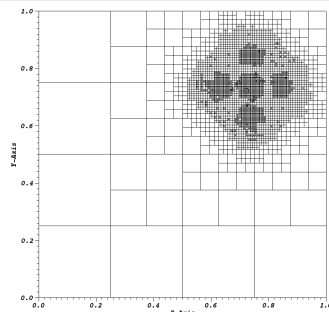
Triangular Sinusoid MMS Results



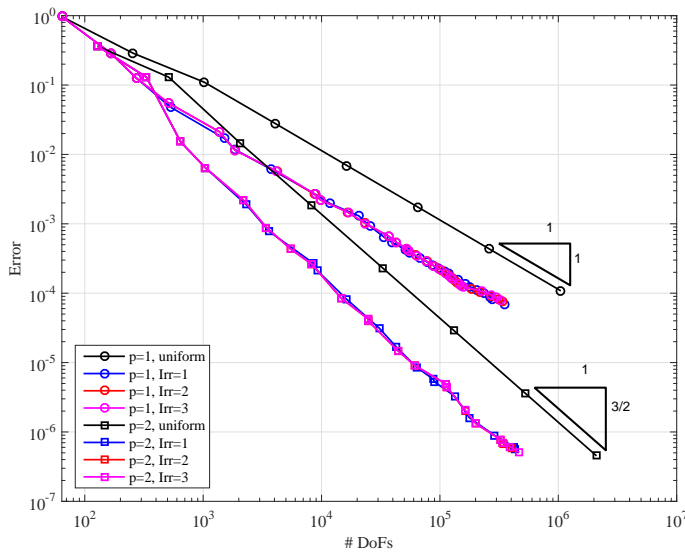
Polygonal Sinusoid MMS Results



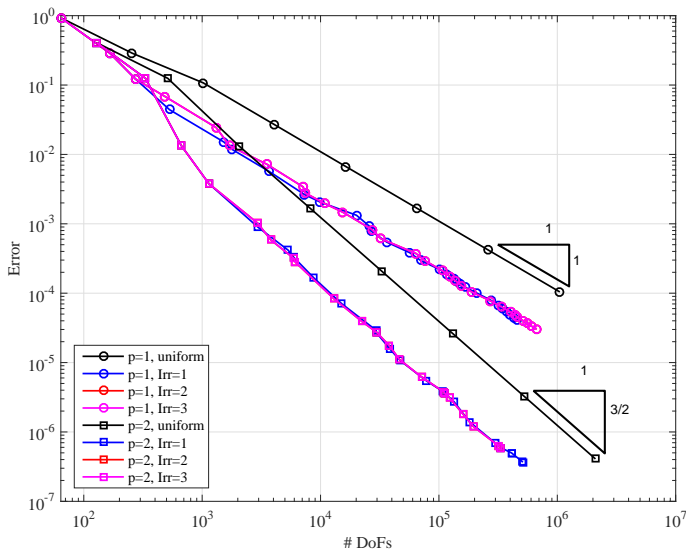
Gaussian AMR - Linear ME cycle 15 (left) and quadratic ME cycle 08 (right)



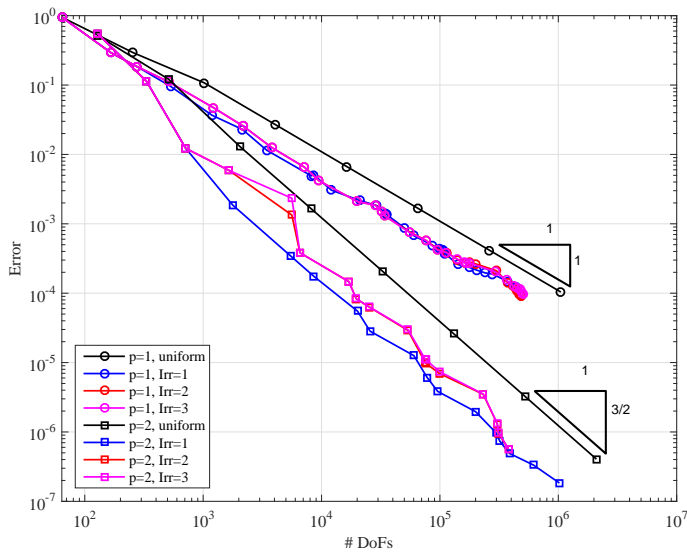
Gaussian MMS Results - PWL



Gaussian MMS Results - Mean Value



Gaussian MMS Results - Maximum Entropy



Purely-Absorbing Material Problem

Solution Regularity Constraint

$$\|\phi - \phi_h\|_{L_2} = C \frac{h^q}{(p+1)^q}, \quad q = \min(p+1, r)$$

r - solution regularity

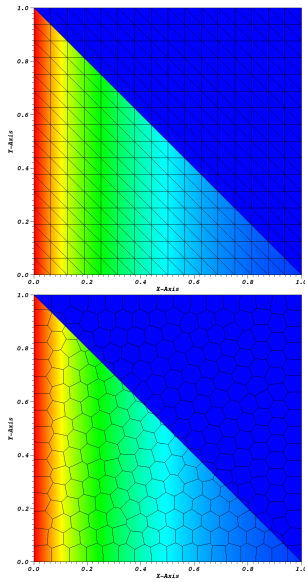
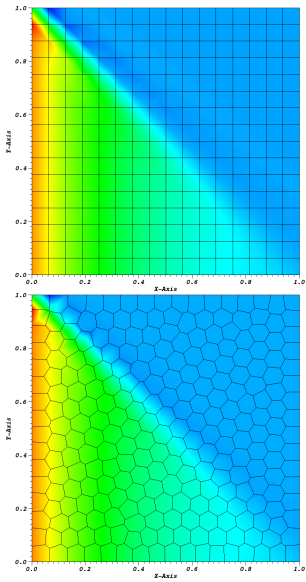
Problem Configuration

- ① Level-Symmetric S_4 quadrature
- ② Incident boundary flux 45°-downwards
 - ① First configuration: left-face incidence only
 - ② Second configuration: left-face and top-face incidence (backup slides)

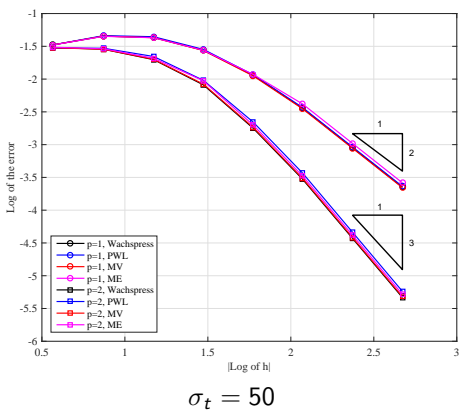
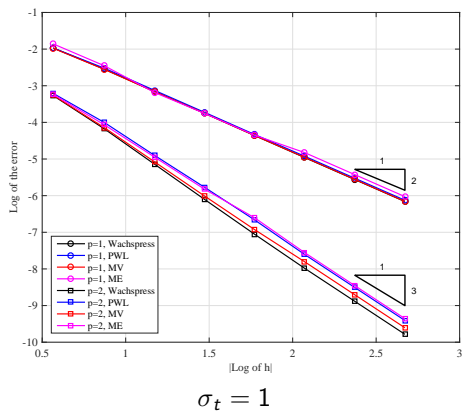
Geometry Configuration

- ① Unit square domain
- ② Cartesian, Triangular, Polygonal, and Split-Polygonal Meshes

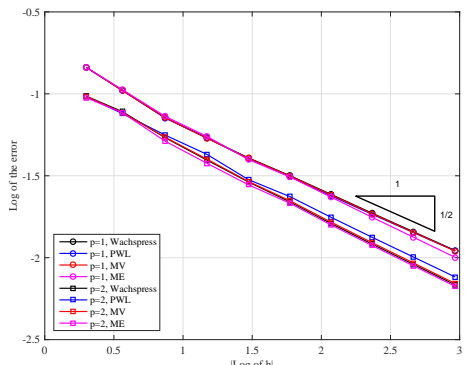
Left-Face Incidence Solutions - $H^{1/2}(\mathcal{D})$



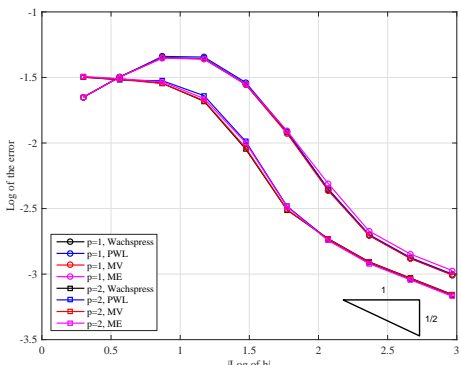
Mesh-Aligned - Left-Face Incidence: $H^{p+1}(\mathcal{D})$



NOT Mesh-Aligned - Left-Face Incidence: $H^{1/2}(\mathcal{D})$



$$\sigma_t = 1$$



$$\sigma_t = 50$$

Thick Diffusion Limit

Sufficient Basis Function Properties for Full Resolution

- Locality of basis function integration on faces
- Surface matching of basis functions across faces

Test Problem

$$\Omega \cdot \nabla \psi + \frac{1}{\epsilon} \psi = \left(\frac{1}{\epsilon} - \epsilon \right) \frac{\phi}{4\pi} + \frac{\epsilon}{4\pi}, \quad \frac{\epsilon}{3} \nabla^2 \phi + \epsilon \phi = \epsilon$$

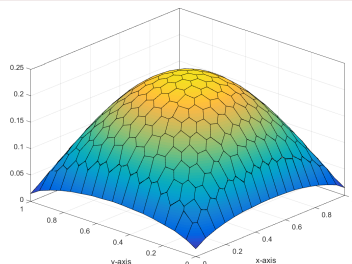
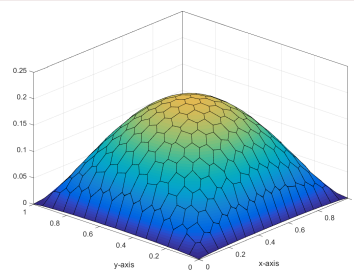
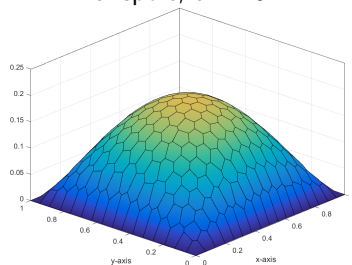
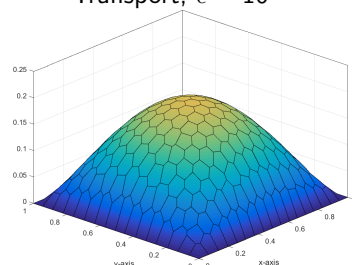
$$\sigma_t \rightarrow \frac{1}{\epsilon} \quad \sigma_a \rightarrow \epsilon \quad \sigma_s \rightarrow \left(\frac{1}{\epsilon} - \epsilon \right) \quad \frac{Q_0}{4\pi} \rightarrow \frac{\epsilon}{4\pi}$$

- Vacuum boundaries
- S_8 level-symmetric quadrature
- CFEM diffusion with “standard” stiffness matrix

Convergence

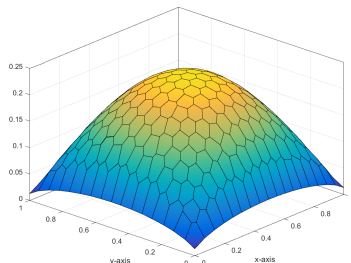
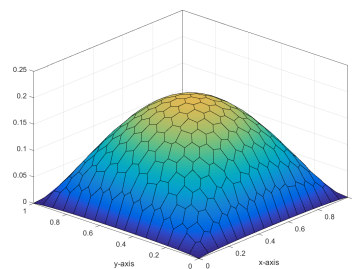
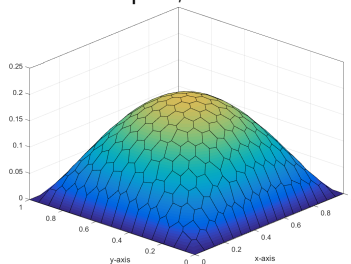
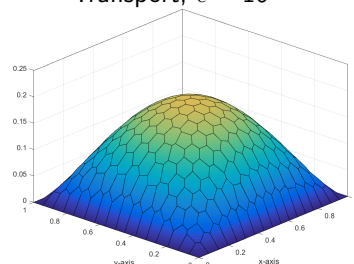
- $\|\phi_D - \phi_T\|_{L_2} \propto \epsilon$
- PWL converges to an alternate diffusion solution

Thick Diffusion Limit - Linear MAXENT

Transport, $\epsilon = 10^{-1}$ Transport, $\epsilon = 10^{-2}$ Transport, $\epsilon = 10^{-3}$ 

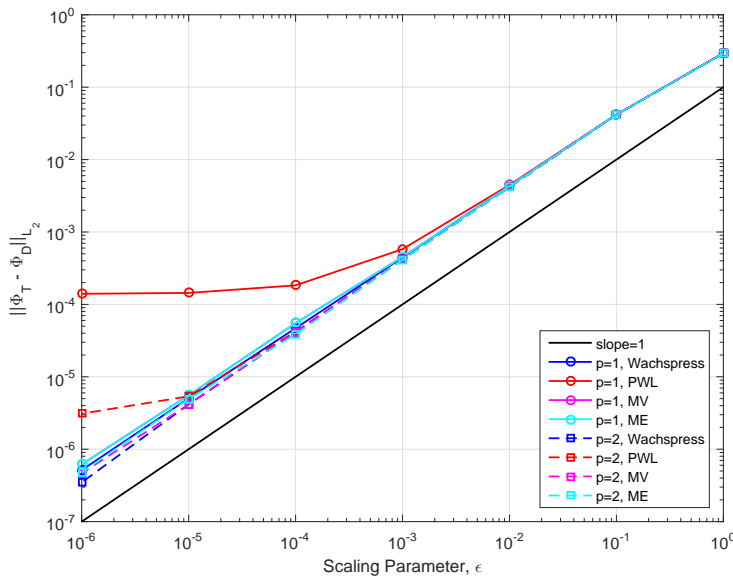
Diffusion

Thick Diffusion Limit - Quadratic MAXENT

Transport, $\epsilon = 10^{-1}$ Transport, $\epsilon = 10^{-2}$ Transport, $\epsilon = 10^{-3}$ 

Diffusion

Polygonal Mesh Convergence Rate



Synthetic Acceleration

Transport sweep and iteration error

$$\begin{aligned} \mathbf{L}\psi^{(\ell+1/2)} &= \mathbf{M}\Sigma\phi^{(\ell)} + \mathbf{Q} & \delta\psi^{(\ell+1/2)} &\equiv \psi - \psi^{(\ell+1/2)} \\ \mathbf{L}\delta\psi^{(\ell+1/2)} &= \mathbf{M}\Sigma\delta\phi^{(\ell+1/2)} + \underbrace{\mathbf{M}\Sigma(\phi^{(\ell+1/2)} - \phi^{(\ell)})}_{\mathbf{R}^{(\ell+1/2)}} & \delta\phi^{(\ell+1/2)} &\equiv \mathbf{D}\delta\psi^{(\ell+1/2)} \end{aligned}$$

Error approximation and update

If we could exactly solve for the error, then the solution could be obtained immediately:

$$\phi^{(\ell+1)} = \phi^{(\ell+1/2)} + \delta\phi^{(\ell+1/2)}$$

However, this is just as difficult as the original transport problem. Instead, we estimate the error using low-order operators:

$$\tilde{\mathbf{A}}\delta\phi^{(\ell+1/2)} = \tilde{\mathbf{R}}^{(\ell+1/2)}$$

$\tilde{\mathbf{A}}$ is a low-order **diffusion** operator.

Various DSA Implementations

Historical DSA Work

- Kopp & Lebedev - independently proposed method
- Gelbard and Hageman (G&B) - efficient convergence on fine meshes
- Reed - showed that G&B diverged for coarse meshes
- Alcouffe - consistency yields efficiency and robustness

Fully-consistent DSA schemes

- Larsen fully-consistent four step
- Fully-consistent DSA (FCDSA)

Partially-consistent DSA schemes

- Modified four step (M4S)
- Waering-Larsen-Adams (WLA)
- Modified Interior Penalty DSA (MIP)

Various DSA Implementations

Historical DSA Work

- Kopp & Lebedev - independently proposed method
- Gelbard and Hageman (G&B) - efficient convergence on fine meshes
- Reed - showed that G&B diverged for coarse meshes
- Alcouffe - consistency yields efficiency and robustness

Fully-consistent DSA schemes

- Larsen fully-consistent four step
- Fully-consistent DSA (FCDSA)

Partially-consistent DSA schemes

- Modified four step (M4S)
- Waering-Larsen-Adams (WLA)
- Modified Interior Penalty DSA (MIP)

Symmetric Interior Penalty (SIP) Form [2]

Bilinear Form

$$\begin{aligned} a(\Phi, b) = & \left\langle D\nabla\Phi, \nabla b \right\rangle_{\mathcal{D}} + \left\langle \sigma\Phi, b \right\rangle_{\mathcal{D}} \\ & + \left\{ \kappa_e^{SIP} [\Phi], [b] \right\}_{E_h^i} - \left\{ [\Phi], \{D\partial_n b\} \right\}_{E_h^i} - \left\{ \{D\partial_n \Phi\}, [b] \right\}_{E_h^i} \\ & + \left\{ \kappa_e^{SIP} \Phi, b \right\}_{\partial\mathcal{D}^d} - \left\{ \Phi, D\partial_n b \right\}_{\partial\mathcal{D}^d} - \left\{ D\partial_n \Phi, b \right\}_{\partial\mathcal{D}^d} + \frac{1}{2} \left\{ \Phi, b \right\}_{\partial\mathcal{D}^r} \end{aligned}$$

Linear Form

$$\begin{aligned} \ell(b) = & \left\langle q, b \right\rangle_{\mathcal{D}} - \left\{ J_0, b \right\}_{\partial\mathcal{D}^n} + 2 \left\{ J_{inc}, b \right\}_{\partial\mathcal{D}^r} \\ & + \left\{ \kappa_e^{SIP} \Phi_0, b \right\}_{\partial\mathcal{D}^d} - \left\{ \Phi_0, D\partial_n b \right\}_{\partial\mathcal{D}^d} \end{aligned}$$

[2] D.N. Arnold. "An interior penalty finite element method with **discontinuous** elements."
SIAM J. Numer. Anal., 19:742-760, (1982).

Symmetric Interior Penalty (SIP) Form

SIP Properties

- Symmetric Positive Definite (SPD)
- Efficiently solved with Preconditioned Conjugate Gradient (PCG) and Algebraic MultiGrid (AMG) preconditioner

SIP Penalty Coefficient

$$\kappa_e^{SIP} \equiv \begin{cases} \frac{C_B}{2} \left(\frac{D^+}{h^+} + \frac{D^-}{h^-} \right) & , e \in E_h^i \\ C_B \frac{D^-}{h^-} & , e \in \partial\mathcal{D} \end{cases}$$

$$C_B = cp(p+1), \quad u^\pm = \lim_{s \rightarrow 0^\pm} u(\mathbf{r} + s\mathbf{n})$$

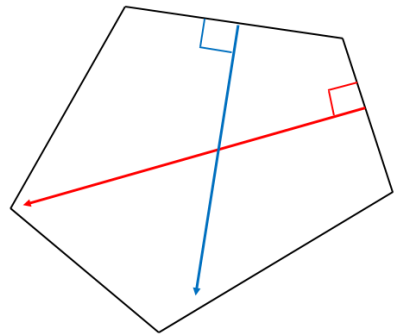
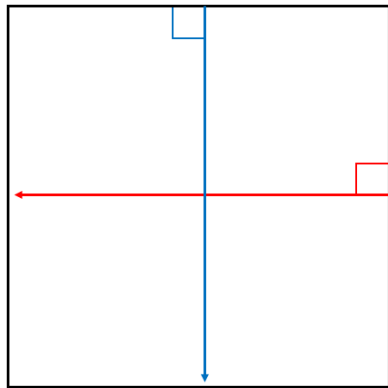
c - user defined constant ($c \geq 1$)

p - polynomial order of the finite element basis (1, 2, 3, ...)

$D^{(+/-)}$ - diffusion coefficient defined on the positive/negative side of a face

$h^{(+/-)}$ - orthogonal projection defined on the positive/negative side of a face

Orthogonal Projection



Modified Interior Penalty (MIP) Form

Recall the DSA equation:

$$\tilde{\mathbf{A}}\delta\phi^{(\ell+1/2)} = \tilde{\mathbf{R}}^{(\ell+1/2)}$$

Diffusion Form

$$\begin{aligned} & \left\langle D\nabla\delta\Phi, \nabla b \right\rangle_{\mathcal{D}} + \left\langle \sigma\delta\Phi, b \right\rangle_{\mathcal{D}} \\ & + \left\{ \kappa_e^{MIP} [\![\delta\Phi]\!], [\![b]\!] \right\}_{E_h^i} - \left\{ [\![\delta\Phi]\!], \{ \{ D\partial_n b \} \} \right\}_{E_h^i} - \left\{ \{ \{ D\partial_n \delta\Phi \} \}, [\![b]\!] \right\}_{E_h^i} \\ & + \left\{ \kappa_e^{MIP} \delta\Phi, b \right\}_{\partial\mathcal{D}^{vac}} - \frac{1}{2} \left\{ \delta\Phi, D\partial_n b \right\}_{\partial\mathcal{D}^{vac}} - \frac{1}{2} \left\{ D\partial_n \delta\Phi, b \right\}_{\partial\mathcal{D}^{vac}} \\ & = \left\langle R, b \right\rangle_{\mathcal{D}} + \left\{ \delta J_{inc}, b \right\}_{\partial\mathcal{D}^{ref}} \end{aligned}$$

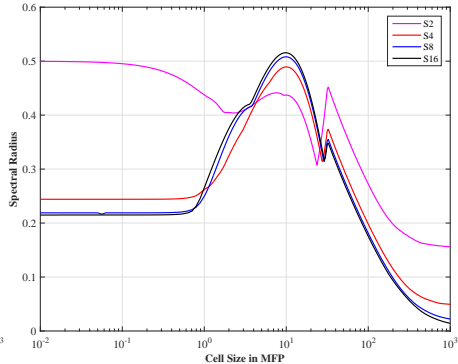
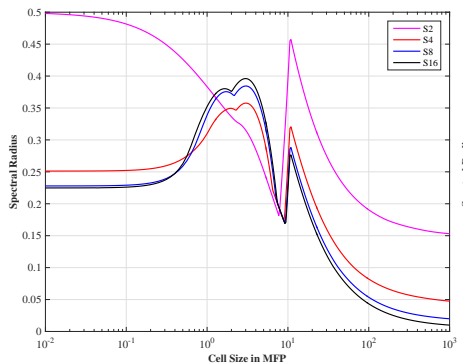
MIP Penalty Term

$$\kappa_e^{MIP} = \max\left(\frac{1}{4}, \kappa_e^{SIP}\right)$$

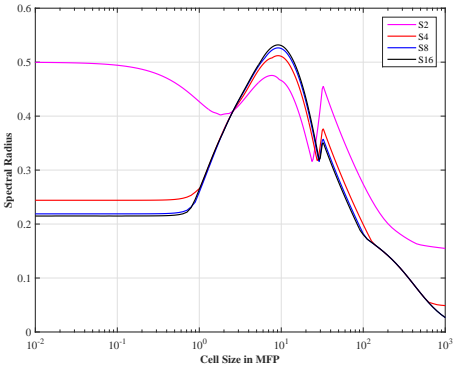
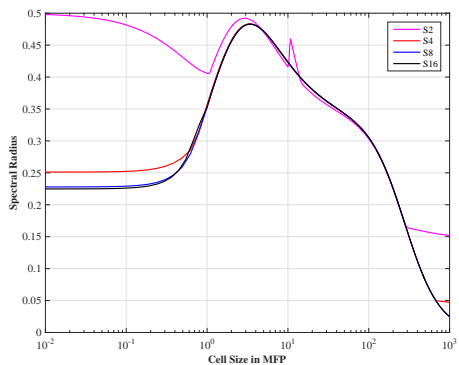
MIP Results Summary

- ① Linear and quadratic 2D basis functions are stable and robust
- ② 3D PWL basis functions
 - ① Stable and robust even on high aspect ratio cells
 - ② Match PDT numerical results well
- ③ Implementation of MIP DSA in PDT
 - ① Scaling suites ran to $O(10^5)$ processors on VULCAN
 - ② DSA fractional times small if given sufficient work for transport sweeps

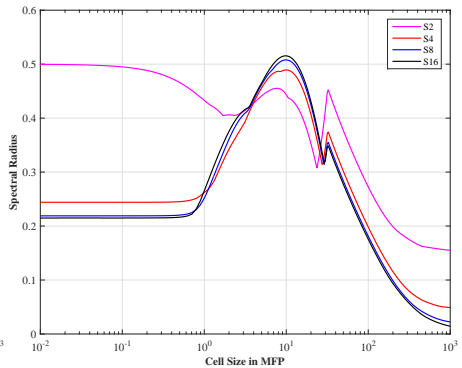
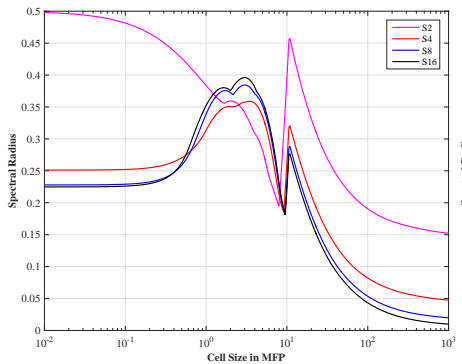
2D Unit Square Fourier Results - linear (left) and quadratic (right) Wachspress



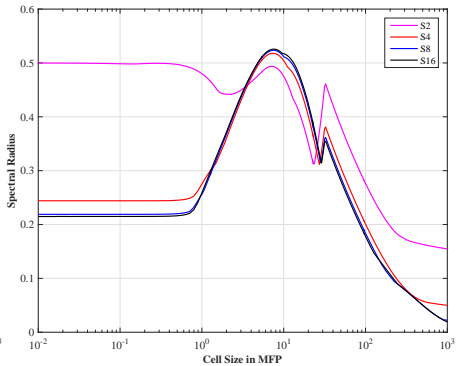
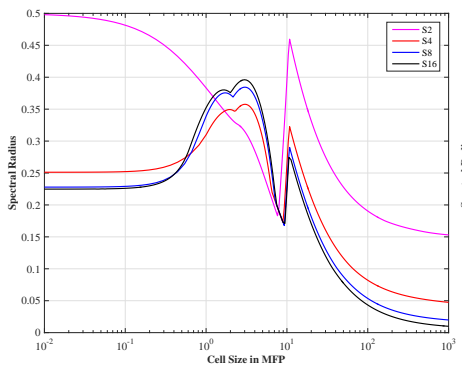
2D Unit Square Fourier Results - linear (left) and quadratic (right) PWL



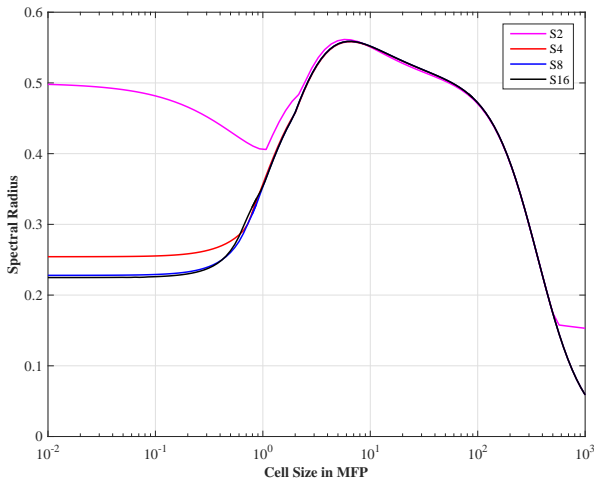
2D Unit Square Fourier Results - linear (left) and quadratic (right) Mean Value



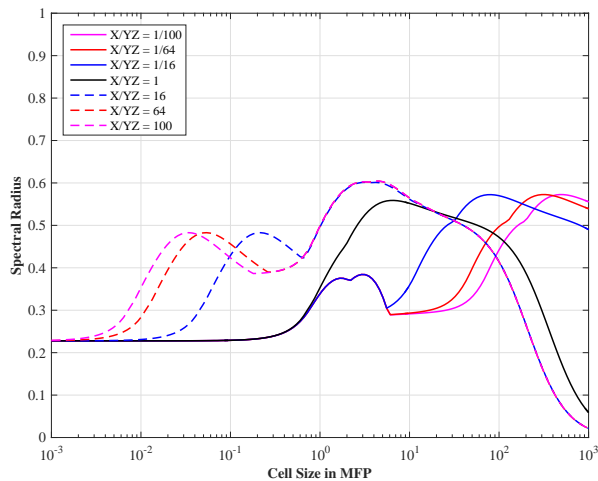
2D Unit Square Fourier Results - linear (left) and quadratic (right) Maximum Entropy



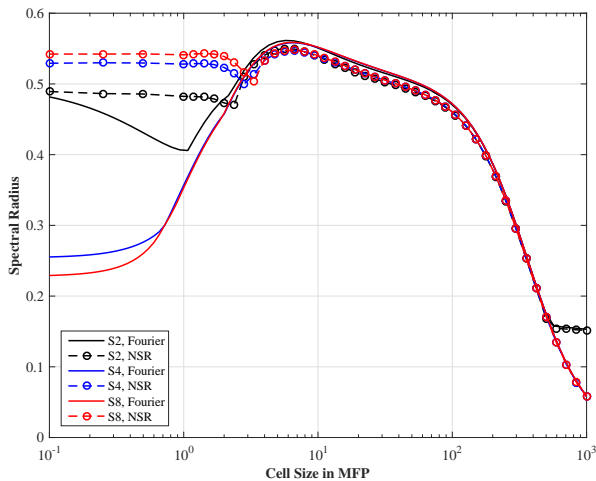
Unit Cube PWL Fourier Analysis



3D PWL Fourier Analysis - Aspect Ratios



Numerical 3D PWL Results



MIP Scaling Results

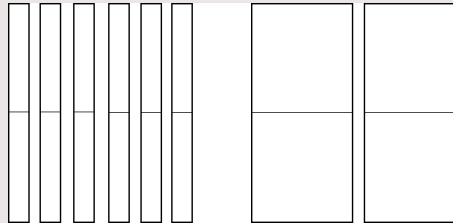
Problem Description

- 1G Zerr problem - used optimal sweep aggregation parameters
- SI precondition with MIP DSA using HYPRE PCG and AMG

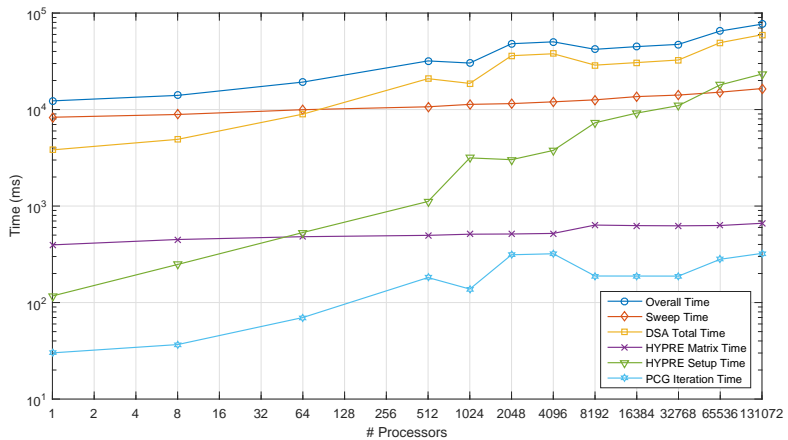
Scaling Suites

- 2 scaling suites - 512 cells/proc and 4096 cells/proc
- Varied number of angles
- 10 SI iterations
- 10 PCG iterations per SI iteration

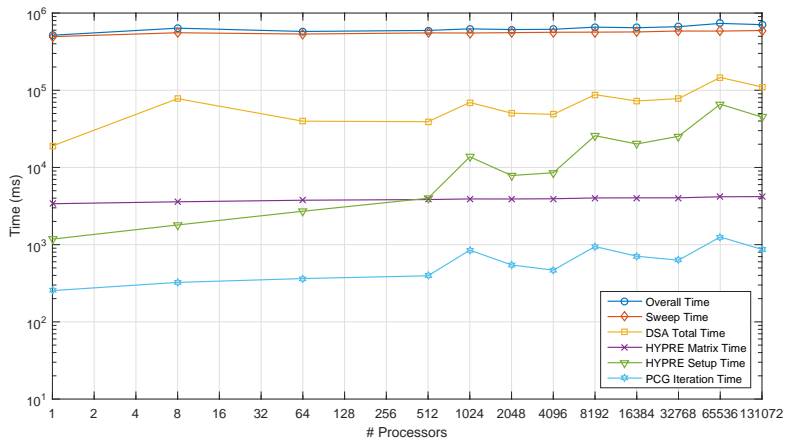
Optimal cell-set configurations



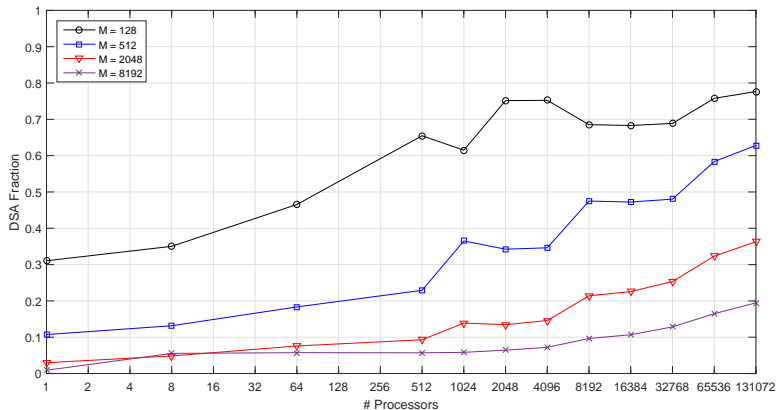
512 cells/processor and 16 angles/octant



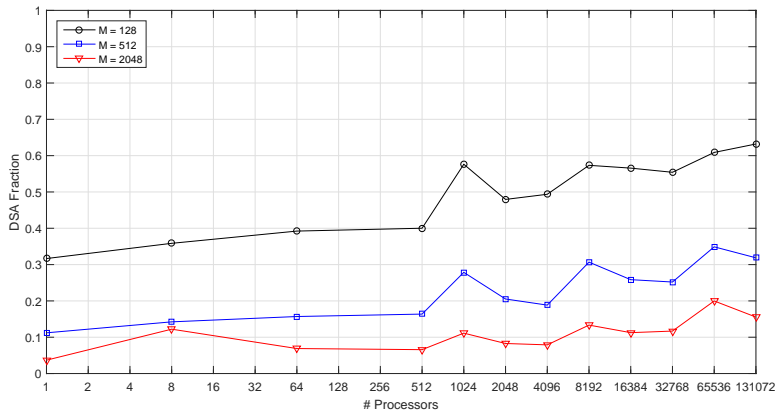
4096 cells/processor and 256 angles/octant



DSA Timing Fraction - 512 cells/processor



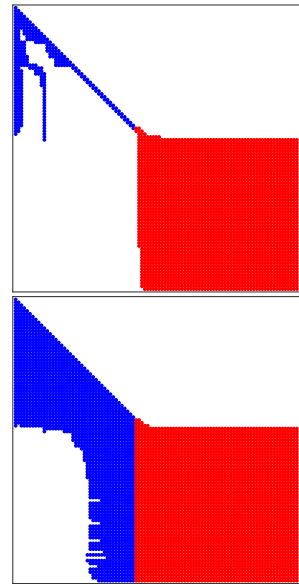
DSA Timing Fraction - 4096 cells/processor



Need for Upscatter Acceleration

Slow Convergence Rates

- Some materials (e.g., graphite and heavy water) have significant thermal neutron upscattering with little absorption
- Can also still have high within-group scattering ratios for $O(10^1)$ - $O(10^2)$ thermal groups
- Simple Gauss-Seidel (in energy) scheme converges slowly
- Need to accelerate outer iterations



Overview of Methods

Multigroup Iteration Schemes

- Gauss-Seidel - sequential (**NOT parallelizable**) iteration of thermal groups
- Jacobi - simultaneous (**parallelizable**) iteration of thermal groups
- Both are poor iterative methods for problems dominated by upscattering

Accelerating Gauss-Seidel - *historical methods*

- Two-Grid Acceleration - DO converge inner iterations
- Modified Two-Grid Acceleration - DO NOT converge inner iterations
- Both perform a spectrally-collapsed diffusion acceleration step

Accelerating Jacobi - *proposed methods*

- Multigroup Jacobi Acceleration
 - DO NOT converge inner iterations
 - Perform a spectrally-collapsed diffusion acceleration step
- Multigroup Jacobi with Inner Acceleration
 - Accelerate within-group iterations with DSA
 - Perform a spectrally-collapsed diffusion acceleration step

Three two-grid-like acceleration methodologies (implemented in PDT)

Standard Two-Grid Acceleration (TG) - Morel 1993

- Gauss Seidel in energy - converging the within-group inner iterations

$$\mathbf{L}_{gg} \psi_g^{(k+1)} = \mathbf{M} \sum_{g'=1}^{\textcolor{blue}{g}} \boldsymbol{\Sigma}_{gg'} \phi_{g'}^{(k+1)} + \mathbf{M} \sum_{g'=\textcolor{red}{g+1}}^G \boldsymbol{\Sigma}_{gg'} \phi_{g'}^{(k)} + \mathbf{Q}_g$$

Modified Two-Grid Acceleration (MTG)

- Do NOT converge the inner iterations

$$\mathbf{L}_{gg} \psi_g^{(k+1)} = \mathbf{M} \sum_{g'=1}^{\textcolor{pink}{g-1}} \boldsymbol{\Sigma}_{gg'} \phi_{g'}^{(k+1)} + \mathbf{M} \sum_{g'=\textcolor{blue}{g}}^G \boldsymbol{\Sigma}_{gg'} \phi_{g'}^{(k)} + \mathbf{Q}_g$$

Multigroup Jacobi Acceleration (MJA)

- Jacobi iterations in energy for some set of energy groups

$$\mathbf{L}_{gg} \psi_g^{(k+1)} = \mathbf{M} \sum_{g'=1}^G \boldsymbol{\Sigma}_{gg'} \phi_{g'}^{(k)} + \mathbf{Q}_g$$

Acceleration Step

- Each of these methods uses a 1-Group energy-collapsed acceleration step.

1-group Energy-Collapsed Diffusion Equation

1G Correction System

- Factorize the error: $\delta\Phi_g^{(k+1/2)} = \xi_g \epsilon^{(k+1/2)}$
- MG Solution Update: $\Phi_g^{(k+1)} = \Phi_g^{(k+1/2)} + \xi_g \epsilon^{(k+1/2)}, \quad \sum_{g=1}^G \xi_g = 1$

$$-\nabla \cdot \langle D \rangle \nabla \epsilon + \langle \sigma \rangle \epsilon = \langle R \rangle$$

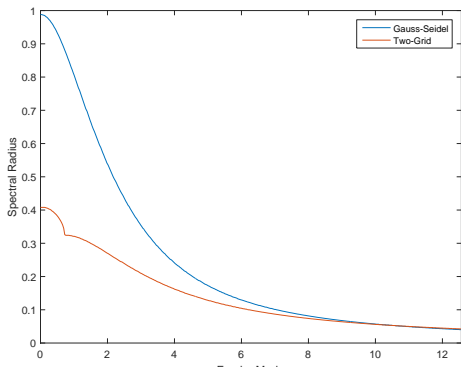
Spectral Distribution and Residual

TG: $(\Sigma_t - S_L - S_D)^{-1} S_U \xi = \rho \xi, \quad \langle R \rangle = \sum_{g=1}^G \left[\sum_{g'=g+1}^G \sigma_{s,0}^{gg'} (\phi_{g,0}^{(k+1/2)} - \phi_{g,0}^{(k)}) \right]$

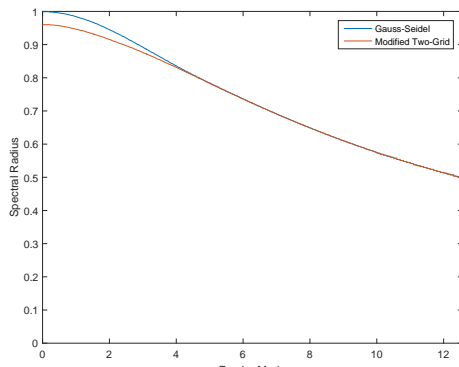
MTG: $(\Sigma_t - S_L)^{-1} (S_D + S_U) \xi = \rho \xi, \quad \langle R \rangle = \sum_{g=1}^G \left[\sum_{g'=g}^G \sigma_{s,0}^{gg'} (\phi_{g,0}^{(k+1/2)} - \phi_{g,0}^{(k)}) \right]$

MJA: $\Sigma_t^{-1} (S_L + S_D + S_U) \xi = \rho \xi, \quad \langle R \rangle = \sum_{g=1}^G \left[\sum_{g'=1}^G \sigma_{s,0}^{gg'} (\phi_{g,0}^{(k+1/2)} - \phi_{g,0}^{(k)}) \right]$

Graphite Fourier Analysis

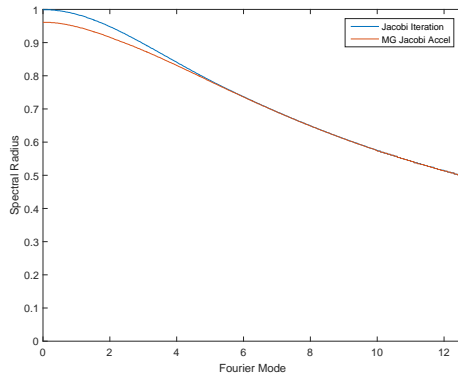


Two-Grid



Modified Two-Grid

Graphite Fourier Analysis



Multigroup Jacobi

Jacobi + Inner Convergence

Iterative Scheme

- ➊ Transport sweep of all G thermal groups: $\mathbf{L}_{gg} \psi_g^{(k+1/3)} = \mathbf{M} \sum_{g'=1}^G \boldsymbol{\Sigma}_{gg'} \phi_{g'}^{(k)} + \mathbf{Q}_g$
- ➋ Parallelizable G within-group DSA steps: $\phi_g^{(k+2/3)} = \phi_g^{(k+1/3)} + \Delta\phi_g^{(k+1/3)}$
- ➌ Energy-collapsed acceleration step: $\phi_g^{(k+1)} = \phi_g^{(k+2/3)} + \xi_g \epsilon^{(k+2/3)}$

 G within-group diffusion solves

$$-\nabla \cdot D_g \nabla \Delta\phi_g^{(k+1/3)} + \sigma_{a,g} \Delta\phi_g^{(k+1/3)} = \sigma_{s,0}^{gg} (\phi_g^{(k+1/3)} - \phi_g^{(k)})$$

Energy-collapsed diffusion step

$$-\nabla \cdot \langle D \rangle \nabla \epsilon^{(k+2/3)} + \langle \sigma \rangle \epsilon^{(k+2/3)} = \langle R^{(k+2/3)} \rangle$$

$$(\boldsymbol{\Sigma}_t - \mathbf{S}_D)^{-1} (\mathbf{S}_L + \mathbf{S}_U) \xi = \rho \xi, \quad \langle R^{(k+2/3)} \rangle = \sum_{g=1}^G \left[\sum_{g' \neq g}^G \sigma_{s,0}^{gg'} (\phi_{g,0}^{(k+2/3)} - \phi_{g',0}^{(k)}) \right]$$

Jacobi + Inner Convergence

Iterative Scheme

- ➊ Transport sweep of all G thermal groups: $\mathbf{L}_{gg} \psi_g^{(k+1/3)} = \mathbf{M} \sum_{g'=1}^G \boldsymbol{\Sigma}_{gg'} \phi_{g'}^{(k)} + \mathbf{Q}_g$
- ➋ Parallelizable G within-group DSA steps: $\phi_g^{(k+2/3)} = \phi_g^{(k+1/3)} + \Delta\phi_g^{(k+1/3)}$
- ➌ Energy-collapsed acceleration step: $\phi_g^{(k+1)} = \phi_g^{(k+2/3)} + \xi_g \epsilon^{(k+2/3)}$

 G within-group diffusion solves

$$-\nabla \cdot D_g \nabla \Delta \phi_g^{(k+1/3)} + \sigma_{a,g} \Delta \phi_g^{(k+1/3)} = \sigma_{s,0}^{gg} (\phi_g^{(k+1/3)} - \phi_g^{(k)})$$

Energy-collapsed diffusion step

$$-\nabla \cdot \langle D \rangle \nabla \epsilon^{(k+2/3)} + \langle \sigma \rangle \epsilon^{(k+2/3)} = \langle R^{(k+2/3)} \rangle$$

$$(\boldsymbol{\Sigma}_t - \mathbf{S}_D)^{-1} (\mathbf{S}_L + \mathbf{S}_U) \xi = \rho \xi, \quad \langle R^{(k+2/3)} \rangle = \sum_{g=1}^G \left[\sum_{g' \neq g}^G \sigma_{s,0}^{gg'} (\phi_{g,0}^{(k+2/3)} - \phi_{g,0}^{(k)}) \right]$$

Jacobi + Inner Convergence

Iterative Scheme

- ➊ Transport sweep of all G thermal groups: $\mathbf{L}_{gg} \psi_g^{(k+1/3)} = \mathbf{M} \sum_{g'=1}^G \boldsymbol{\Sigma}_{gg'} \phi_{g'}^{(k)} + \mathbf{Q}_g$
- ➋ Parallelizable G within-group DSA steps: $\phi_g^{(k+2/3)} = \phi_g^{(k+1/3)} + \Delta\phi_g^{(k+1/3)}$
- ➌ Energy-collapsed acceleration step: $\phi_g^{(k+1)} = \phi_g^{(k+2/3)} + \xi_g \epsilon^{(k+2/3)}$

 G within-group diffusion solves

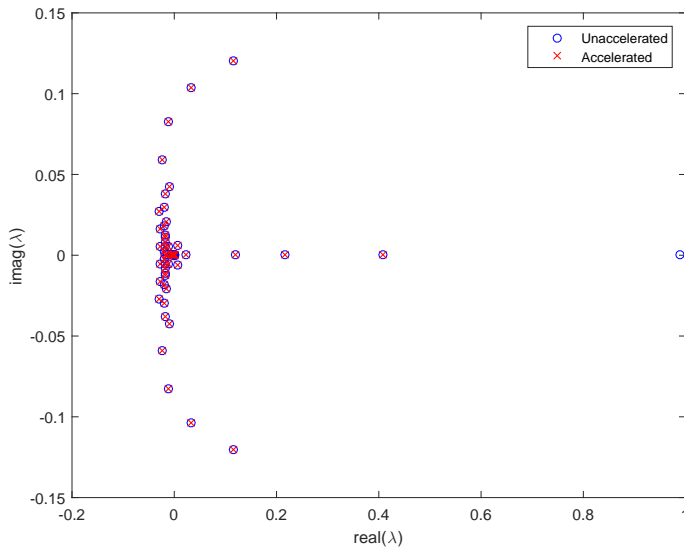
$$-\nabla \cdot D_g \nabla \Delta \phi_g^{(k+1/3)} + \sigma_{a,g} \Delta \phi_g^{(k+1/3)} = \sigma_{s,0}^{gg} (\phi_g^{(k+1/3)} - \phi_g^{(k)})$$

Energy-collapsed diffusion step

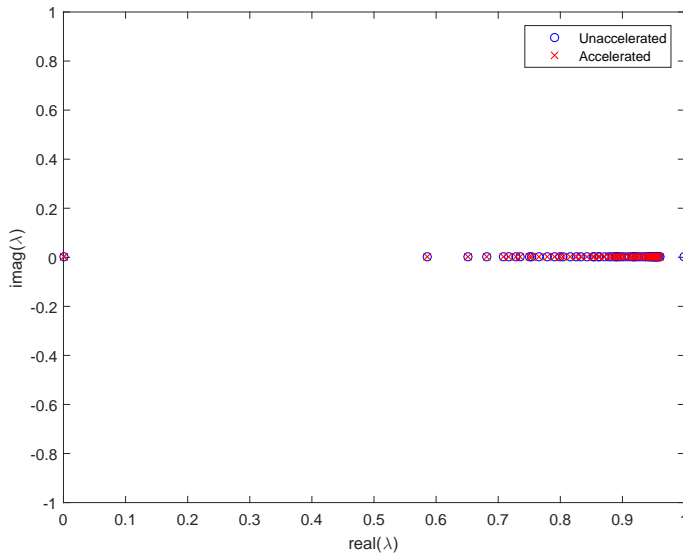
$$-\nabla \cdot \langle D \rangle \nabla \epsilon^{(k+2/3)} + \langle \sigma \rangle \epsilon^{(k+2/3)} = \langle R^{(k+2/3)} \rangle$$

$$(\mathbf{\Sigma}_t - \mathbf{S}_D)^{-1} (\mathbf{S}_L + \mathbf{S}_U) \xi = \rho \xi, \quad \langle R^{(k+2/3)} \rangle = \sum_{g=1}^G \left[\sum_{g' \neq g}^G \sigma_{s,0}^{gg'} (\phi_{g,0}^{(k+2/3)} - \phi_{g,0}^{(k)}) \right]$$

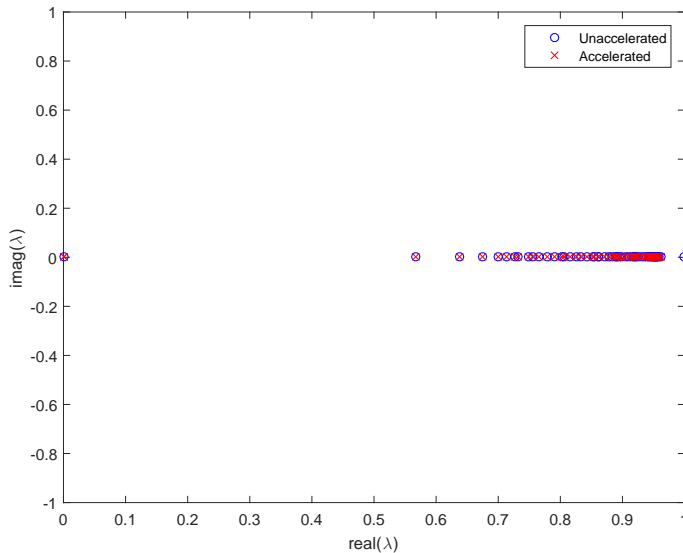
Graphite Two-Grid (TG) Flat Mode Eigenvalues



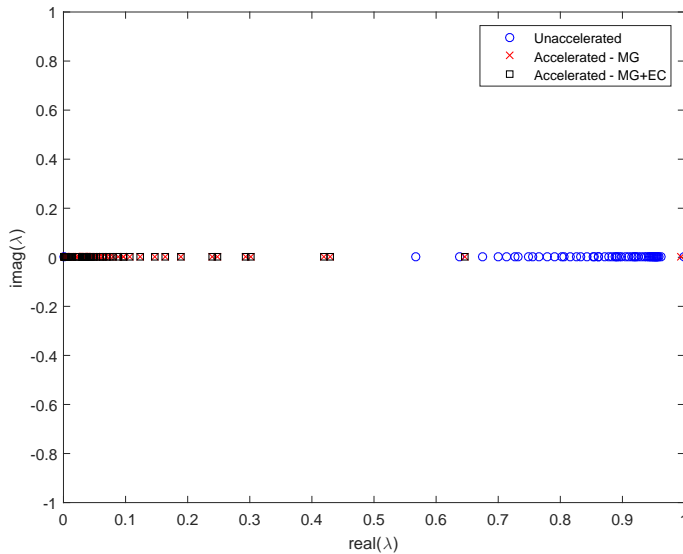
Graphite Modified Two-Grid (MTG) Flat Mode Eigenvalues



Graphite Multigroup Jacobi Acceleration (MJA) Flat Mode Eigenvalues



Graphite Multigroup Jacobi with Inner Acceleration (MJIA) Flat Mode Eigenvalues

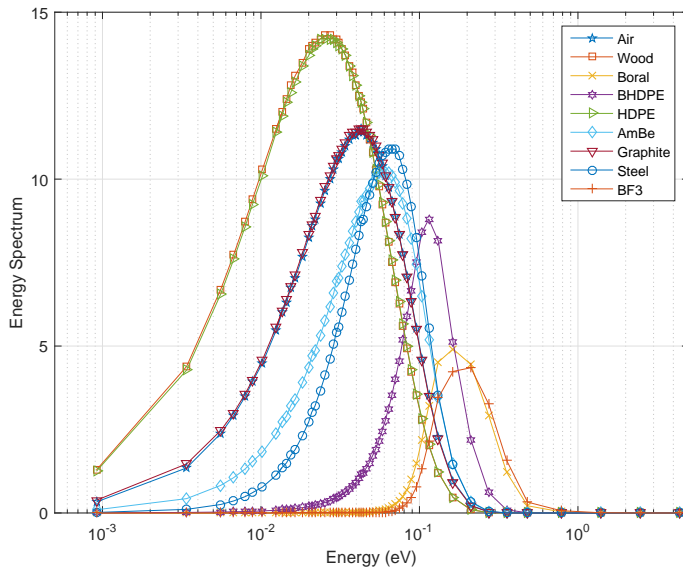


IM1 Problem

- Calibration of impurities in graphite bars
- 99 energy groups - 42 fast and 57 thermal
- Fast groups organized into 11 group sets
- Other materials include HDPE, Borated-HDPE, wood, air, AmBe, BF₃, Boral, and steel



IM1 Two-Grid Spectral Shapes



Infinite Medium Fourier Results

Material	U. TG	A. TG	U. MTG	A. MTG	U. MJA	A. MJA	A. MJIA
Graphite	0.9883	0.4084	0.9993	0.9604	0.9993	0.9613	0.6462
HDPE	0.8916	0.4343	0.9918	0.7527	0.9943	0.8015	0.6631
B-HDPE	0.0258	0.0177	0.1331	0.1221	0.1336	0.1223	0.0639
Wood	0.9820	0.2101	0.9840	0.3836	0.9915	0.5326	0.4684
AmBe	0.4835	0.2724	0.5646	0.5554	0.7068	0.5596	0.4947
Steel	0.6989	0.5809	0.9243	0.9215	0.9255	0.9215	0.7547
Boral	0.0023	0.0016	0.0782	0.0602	0.0782	0.0602	0.0039
BF3	0.0008	0.0006	0.0351	0.0266	0.0351	0.0266	0.0086
Air	0.7580	0.5282	0.8121	0.7828	0.8845	0.7896	0.7166

2D Variant Results

Two-Grid Results - 10^{-7} inner tolerance

Problem	Outer Iter.	1-Group Sweeps	Solve Time (min)
SI	361	185,422	486.50
SI+DSA	55	35,699	96.48
GMRES	38	41,575	128.63
GMRES+DSA	14	19,053	57.92

Modified Two-Grid Results

Problem	Outer Iter.	1-Group Sweeps	Solve Time (min)
SI	536	77,632	275.83
SI+DSA	73	10,846	40.60
GMRES	78	4,845	25.82
GMRES+DSA	26	1,881	11.09

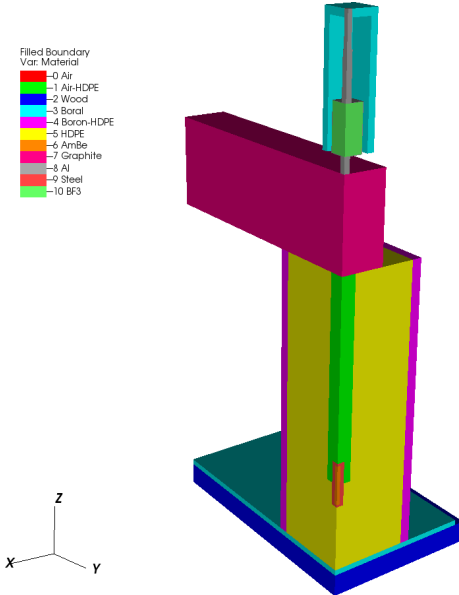
Multigroup Jacobi Results

Problem	Outer Iter.	1-Group Sweeps	Solve Time (min)
SI	1,734	98,838	111.07
SI+DSA	157	8,949	15.49
GMRES	118	6,726	8.65
GMRES+DSA	35	1,995	4.16

3D IM1 Results

Filled Boundary
Var. Material

- 0 Air
- 1 Air-HDPE
- 2 Wood
- 3 Boral
- 4 Boron-HDPE
- 5 HDPE
- 6 AmBe
- 7 Graphite
- 8 Al
- 9 Steel
- 10 BF3



3D IM1 Results

Two-Grid Results

Problem	Outer Iter.	1-Group Sweeps	Solve Time (hr)
SI	-	-	-
SI+DSA	-	-	-
GMRES	-	-	-
GMRES+DSA	14	11,104	32.5*

Modified Two-Grid Results

Problem	Outer Iter.	1-Group Sweeps	Solve Time (hr)
SI	-	-	-
SI+DSA	-	-	-
GMRES	81	4,617	14.2*
GMRES+DSA	34	1,938	4.82

Multigroup Jacobi Results

Problem	Outer Iter.	1-Group Sweeps	Solve Time (hr)
SI	-	-	-
SI+DSA	256	14,592	11.2
GMRES	120	6,840	4.93
GMRES+DSA	31	1,767	1.76

Conclusions

POLYFEM Conclusions

- ① Investigated four linearly-complete polygonal basis functions: Wachspress, PWL, Mean Value, and Maximum Entropy
- ② Conversion to quadratic serendipity space of functions
- ③ Satisfies properties for the thick diffusion limit
- ④ H^{p+1} convergence for regular transport solutions
- ⑤ $H^{1/2}$ convergence for irregular discontinuous solutions
- ⑥ $H^{3/2}$ convergence for irregular continuous solutions (in backup)

DSA Conclusions

- ① MIP is stable and robust for 3D DSA problems
- ② MIP scheme - SPD and efficiently solved with PCG and AMG preconditioning
- ③ MIP implemented in PDT - good scaling out to $O(10^5)$ processors
- ④ Proposed MJA and MJIA methods - parallelizable
- ⑤ MJA numerically shown to yield better wallclock times than traditional upscatter acceleration methods

Conclusions

POLYFEM Conclusions

- ① Investigated four linearly-complete polygonal basis functions: Wachspress, PWL, Mean Value, and Maximum Entropy
- ② Conversion to quadratic serendipity space of functions
- ③ Satisfies properties for the thick diffusion limit
- ④ H^{p+1} convergence for regular transport solutions
- ⑤ $H^{1/2}$ convergence for irregular discontinuous solutions
- ⑥ $H^{3/2}$ convergence for irregular continuous solutions (in backup)

DSA Conclusions

- ① MIP is stable and robust for 3D DSA problems
- ② MIP scheme - SPD and efficiently solved with PCG and AMG preconditioning
- ③ MIP implemented in PDT - good scaling out to $O(10^5)$ processors
- ④ Proposed MJA and MJIA methods - parallelizable
- ⑤ MJA numerically shown to yield better wallclock times than traditional upscatter acceleration methods

Open Items

POLYFEM Open Items

- ① Quadratic serendipity basis functions on 3D polyhedra
- ② Higher-order 2D serendipity polygonal basis functions
- ③ Alternative integration schemes on polygons

DSA Open Items

- ① Numerical implementation and verification of the MJIA method
- ② Mixed-mode parallelism with DSA preconditioning

Thank you!

Questions?

A special acknowledgment to the Department of Energy Rickover Fellowship Program in Nuclear Engineering, which provides strong support to its fellows and their professional development.



TEXAS A&M★
ENGINEERING

A matrix constraints

Constant Constraint

$$\sum_{ii \in V} c_{aa}^{ii} + \sum_{i(i+1) \in E} 2c_{aa}^{i(i+1)} = 1, \quad \forall aa \in V$$

$$\sum_{ii \in V} c_{ab}^{ii} + \sum_{i(i+1) \in E} 2c_{ab}^{i(i+1)} = 2, \quad \forall ab \in E \cup D$$

Linear Constraint

$$\sum_{ii \in V} c_{aa}^{ii} \mathbf{x}_{ii} + \sum_{i(i+1) \in E} 2c_{aa}^{i(i+1)} \mathbf{x}_{i(i+1)} = \mathbf{x}_{aa}, \quad \forall aa \in V$$

$$\sum_{ii \in V} c_{ab}^{ii} \mathbf{x}_{ii} + \sum_{i(i+1) \in E} 2c_{ab}^{i(i+1)} \mathbf{x}_{i(i+1)} = 2\mathbf{x}_{ab}, \quad \forall ab \in E \cup D$$

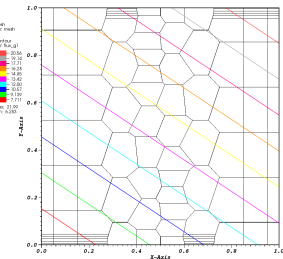
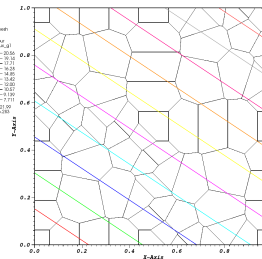
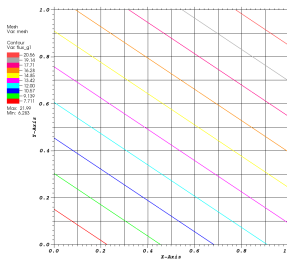
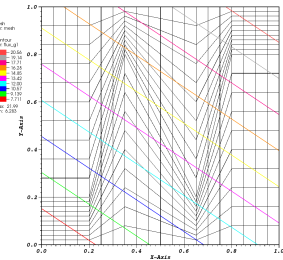
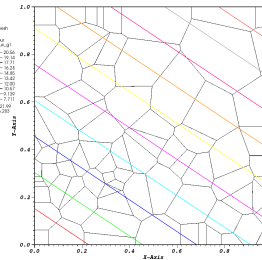
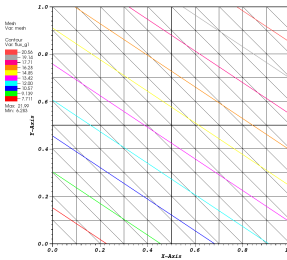
Quadratic Constraint

$$\sum_{ii \in V} c_{aa}^{ii} \mathbf{x}_i \mathbf{x}_i^T + \sum_{i(i+1) \in E} c_{aa}^{i(i+1)} (\mathbf{x}_i \mathbf{x}_{i+1}^T + \mathbf{x}_{i+1} \mathbf{x}_i^T) = \mathbf{x}_a \mathbf{x}_a^T, \quad \forall aa \in V$$

$$\sum_{ii \in V} c_{ab}^{ii} \mathbf{x}_i \mathbf{x}_i^T + \sum_{i(i+1) \in E} c_{ab}^{i(i+1)} (\mathbf{x}_i \mathbf{x}_{i+1}^T + \mathbf{x}_{i+1} \mathbf{x}_i^T) = \mathbf{x}_a \mathbf{x}_b^T + \mathbf{x}_b \mathbf{x}_a^T, \quad \forall ab \in E \cup D$$

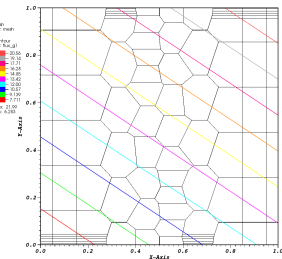
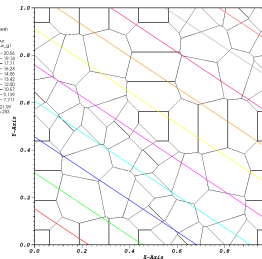
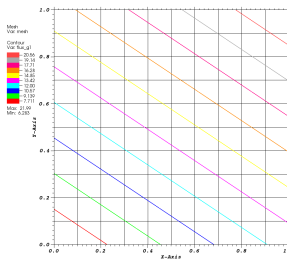
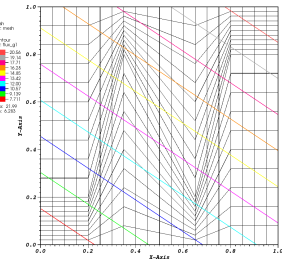
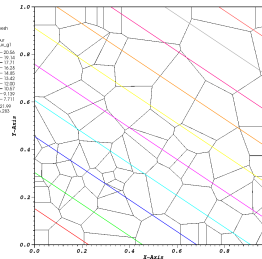
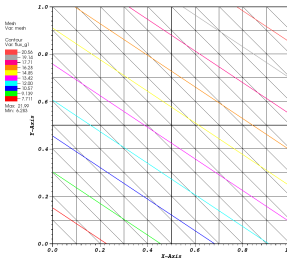


Exactly-Linear Transport Solutions - Wachspress



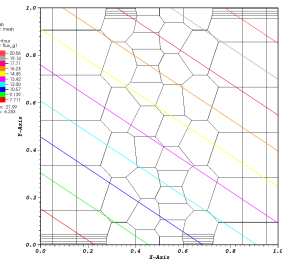
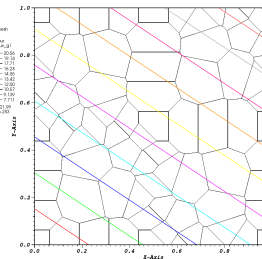
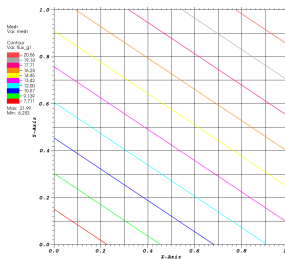
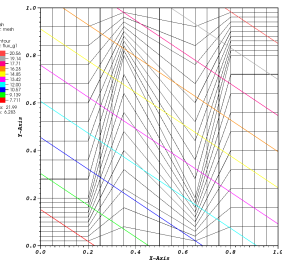
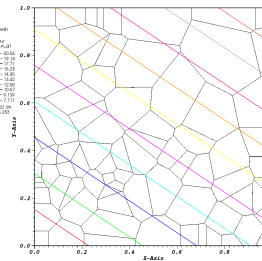
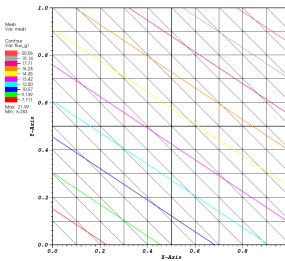


Exactly-Linear Transport Solutions - PWL



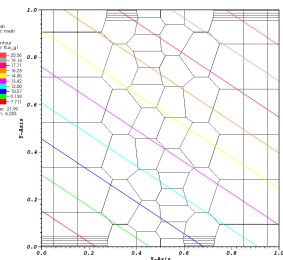
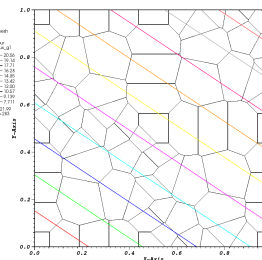
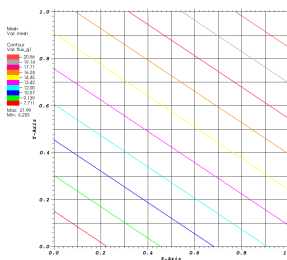
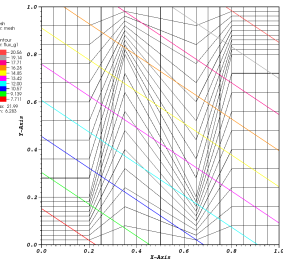
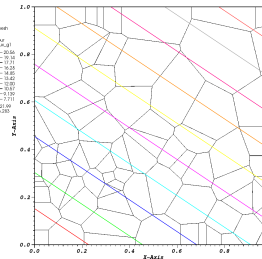
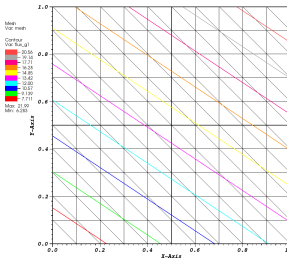


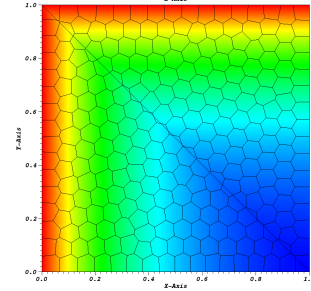
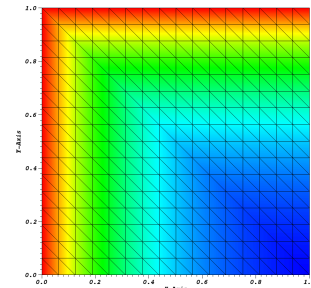
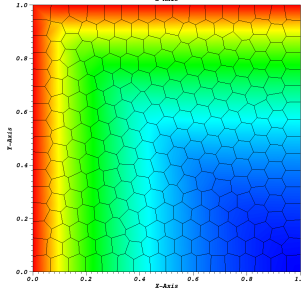
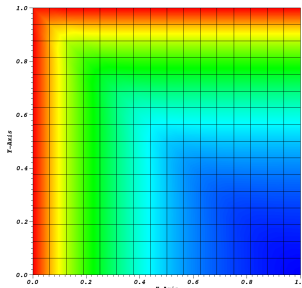
Exactly-Linear Transport Solutions - Mean Value



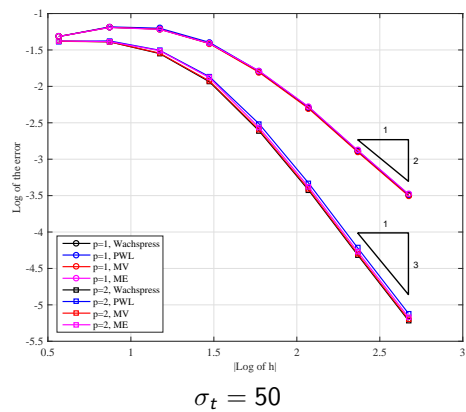
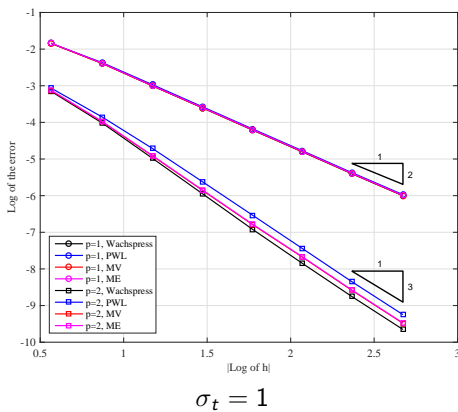


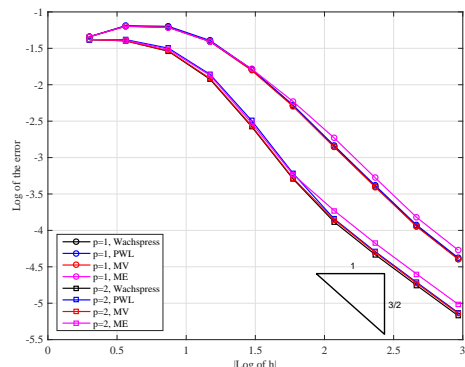
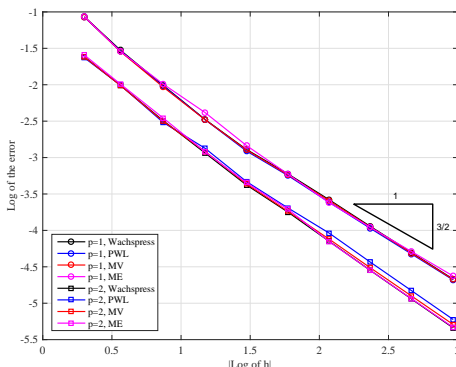
Exactly-Linear Transport Solutions - MAXENT



Left-Face Incidence Solutions - $H^{1/2}(\mathcal{D})$ 

Mesh-Aligned - Left-Face and Top-Face Incidence: $H^{p+1}(\mathcal{D})$



NOT Mesh-Aligned - Left-Face and Top-Face Incidence: $H^{3/2}(\mathcal{D})$ 

Orthogonal Projection

2D Orthogonal Projections

Number of Vertices	3	4	> 4 and even	> 4 and odd
h	$2 \frac{A_K}{L_f}$	$\frac{A_K}{L_f}$	$4 \frac{A_K}{P_K}$	$2 \frac{A_K}{P_K} + \sqrt{\frac{2A_K}{N_K \sin(\frac{2\pi}{N_K})}}$

N_K - # of vertices for polygon K

A_K - Area of polygon K

L_f - Length of face f

P_K - Perimeter for polygon K

3D Orthogonal Projections

Number of Faces	4	6	otherwise
h	$3 \frac{V_K}{A_f}$	$\frac{V_K}{A_f}$	$6 \frac{V_K}{SA_K}$

V_K - Volume of polyhedron K

A_f - Area of face f

SA_K - Surface area of polyhedron K

Linear Basis Functions on 3D Polyhedra

Linear basis functions and convex polyhedra only for 3D

- The 2D quadratic serendipity formulation is more arduous in 3D
- Intercell coupling is not straightforward for concave polyhedra
- Focus on 3D PWL functions
- Focus on 3D parallelepipeds and extruded convex polygons (convex prisms)

3D PWL basis functions

$$b_i(\mathbf{x}) = t_i(\mathbf{x}) + \sum_{f=1}^{F_i} \beta_f^i t_f(\mathbf{x}) + \alpha_i t_c(\mathbf{x})$$

t_i - standard 3D linear function for a tet ($i, i+1, f_c, K_c$); 1 at vertex i , linearly decreases to 0 to the cell center, each adjoining face center, and each adjoining vertex

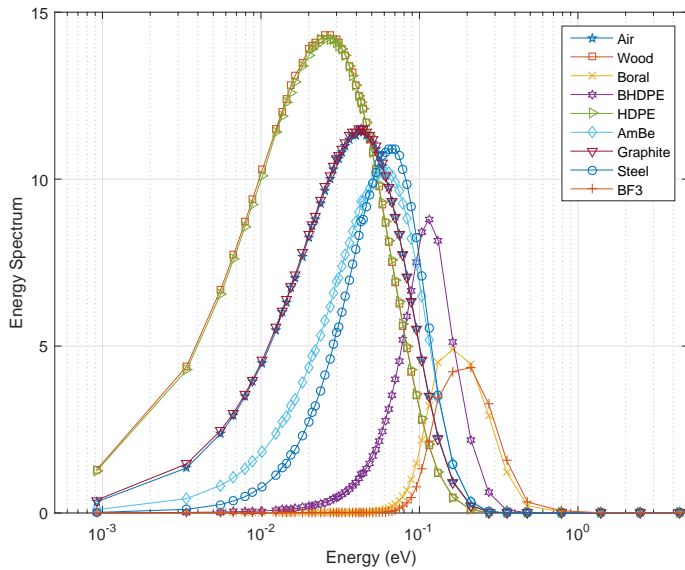
t_c - 3D tent function; 1 at cell center, linearly decreases to 0 at all vertices and face centers

t_f - face tent function; 1 at face center, linearly decreases to 0 at each face vertex and cell center

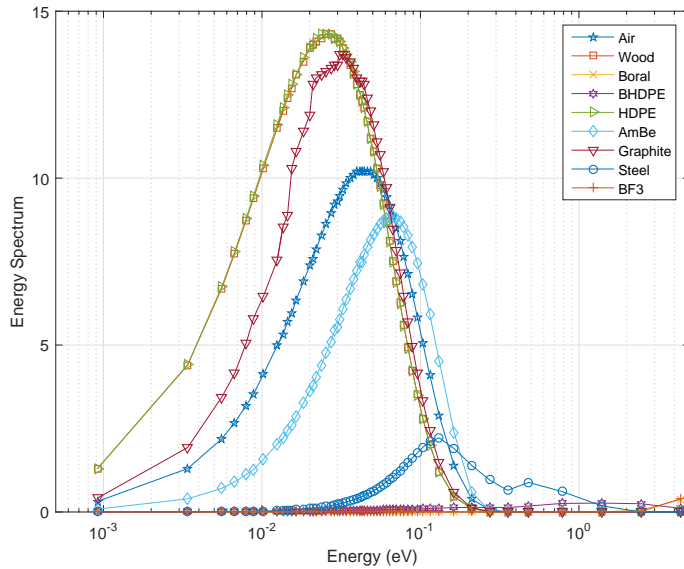
$\alpha_i = \frac{1}{N_V}$ - weight parameter for vertex i

$\beta_f^i = \frac{1}{N_f}$ - weight parameter for face f touching vertex i

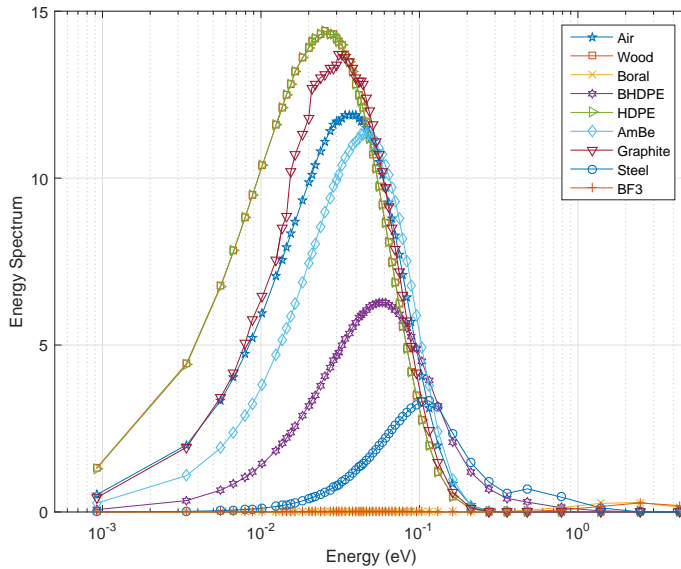
IM1 Two-Grid Spectral Shapes



IM1 Modified Two-Grid Spectral Shapes



IM1 Multigroup Jacobi Acceleration Spectral Shapes



IM1 Multigroup Jacobi with Inner Acceleration Spectral Shapes

